

# Subcooling methods for CO<sub>2</sub> refrigeration cycles. A Review.

Rodrigo Llopis\*, Laura Nebot-Andrés, Daniel Sánchez, Jesús Catalán-Gil, Ramón Cabello

Thermal Engineering Group, Mechanical Engineering and Construction Department,  
Jaume I University, Spain

\*Corresponding author: [rllopis@uji.es](mailto:rllopis@uji.es), +34 964 718136

## Abstract

CO<sub>2</sub> subcooling has resulted a method to upgrade the performance of CO<sub>2</sub> refrigeration plants in the recent years, with overall improvements up to 12% with internal heat exchangers, 22% with economizers, 25.6% with thermoelectric systems and 30.3% with dedicated subcooling methods. This paper comprehensively reviews the recent studies that consider subcooling as a way to upgrade the performance of CO<sub>2</sub> refrigeration cycles. The review is limited to CO<sub>2</sub> refrigeration cycles with accumulation receiver for commercial purposes and does not consider air conditioning or MAC systems. It is organized as follows: first, the thermodynamic aspects of subcooling in CO<sub>2</sub> refrigeration cycles are described and discussed; second, the main results and conclusions of the recent investigations are analysed inside two big groups: subcooling internal methods and subcooling external methods. Finally, the review synthesizes the current state of the art and points out the lines of research that deserve future developments.

## Highlights

- Research using subcooling as way to improve CO<sub>2</sub> refrigeration is analysed.
- COP improvements up to 37.8% of CO<sub>2</sub> base systems have been reported.
- State-of-the art subcooling systems are presented and discussed
- New opportunities for research are highlighted in the review.

## Keywords

CO<sub>2</sub>; subcooling; dedicated mechanical subcooling; integrated mechanical subcooling; thermoelectric subcooling

## Index

Abstract.....	1
Nomenclature .....	3
1. Introduction .....	5
2. Thermodynamic aspects of CO <sub>2</sub> subcooling .....	7
2.1. Summary of CO <sub>2</sub> properties.....	7
2.2. Cycle with subcooling and operation .....	8
2.2.1. Subcooling in subcritical conditions.....	9
2.2.2. Subcooling in transcritical conditions .....	10
2.3. Benefits of subcooling .....	12
2.3.1. Capacity .....	13
2.3.2. COP .....	15
2.4. Energy required by the subcooling system (cost of subcooling).....	16
2.5. Optimization of subcooling .....	17
3. Internal methods .....	18
3.1. Internal Heat Exchanger (IHX) .....	18
3.1.1 Classical positions.....	18
3.1.2. Combination of the IHX with ejectors .....	22
3.1.3. Combination of the IHX with expanders.....	23
3.1.4. IHX with vapour extraction from the intermediate vessel .....	24
3.2. Economizer or subcooler.....	25
3.3. Integrated Mechanical subcooler.....	26
3.4. Heat storage systems.....	28
4. Dedicated subcooling methods.....	29
4.1. Dedicated mechanical subcooling (DMS).....	29
4.2. Thermoelectric subcooling systems (TSS) .....	33
4.3. Other hybrid systems.....	35
5. Concluding remarks.....	36
6. References .....	38

## Nomenclature

<i>BP</i>	back-pressure
<i>COND</i>	condenser
<i>COP</i>	coefficient of performance
<i>EJ</i>	ejector
<i>EV</i>	evaporator
<i>GC</i>	gas-cooler/condenser
<i>GWP</i>	global warming potential
<i>h</i>	specific enthalpy, J·kg <sup>-1</sup>
<i>IHX</i>	internal heat exchanger
<i>MAC</i>	mobile air conditioning system
$\dot{m}_r$	refrigerant mass flow rate, kg·s <sup>-1</sup>
<i>p</i>	pressure, bar
<i>P<sub>C</sub></i>	electric power consumption, W
<i>P<sub>C,sub</sub></i>	electric power consumption of the subcooling system, W
$\dot{Q}$	heat transfer rate, W
<i>q</i>	specific enthalpy difference, J·kg <sup>-1</sup>
<i>Rec</i>	receiver
<i>RICOSP</i>	ratio of increase in capacity related to subcooling capacity
<i>SUB</i>	subcooling degree, K
<i>SH</i>	superheating degree at evaporator, K
<i>t</i>	temperature, °C
<i>TEV</i>	thermostatic expansion valve
<i>TSS</i>	thermoelectric subcooling system
<i>w<sub>C</sub></i>	specific compression work, J·kg <sup>-1</sup>
<i>x<sub>v</sub></i>	vapour quality

### Greek symbols

$\Delta$	increment
$\eta$	efficiency

$\varepsilon$  thermal effectiveness

### Subscripts

*air* air

*AUX* auxiliary compressor

*base* base line system

*C* cold source level, critical point condition

*crit* critical point conditions

*dep* accumulation vessel

*eje* ejector

*env* environment

*exp* expander

*gc* gas-cooler/condenser

*H* hot sink level

*I* intermediate temperature level

*IHX* internal heat exchanger

*in* inlet

*K* condenser

*MAIN* main compressor

*O* evaporator

*out* outlet

*PS* pseudocritical temperature

*s* isentropic process

*sub* subcooler, subcooling device, subcooling

*w* water, secondary fluid

# 1. Introduction

CO<sub>2</sub> refrigeration systems were rescued by Prof. Lorentzen (1994) in the nineties as a reasonable and technical possible solution to replace artificial refrigerants in air conditioning and refrigeration applications. As Lorentzen and Pettersen stated, implementation of CO<sub>2</sub> cycles would avoid '*continued emissions of several hundred thousand tonnes of alien chemicals to the atmosphere each year, involving the potential risk of unforeseen environmental effects*' (Lorentzen and Pettersen, 1993).

Renaissance of CO<sub>2</sub> as working fluid for refrigerant applications was slow, because the initial CO<sub>2</sub> refrigeration systems, especially those working or analysed in transcritical conditions, reached an energy efficiency level not comparable to that of artificial refrigerants. To solve the problem, the scientific community did great effort on the last decades. First, research was focused on defining alternative refrigeration schemes and on improving the performance of individual components (Groll and Kim, 2007; Kim et al., 2004). This initial stage of research clearly showed that the working schemes of competitive plants would be very different from the traditional schemes used with artificial refrigerants, owing that CO<sub>2</sub> refrigeration requires a devoted control of the heat rejection pressure in transcritical conditions (Peñarrocha et al., 2014). Second, CO<sub>2</sub> refrigeration was taken a step forward due to the development of expanders (Singh and Dasgupta, 2016) and ejector systems (Elbel, 2011; Elbel and Lawrence, 2016; Hafner et al., 2014), which allowed to recover energy in the expansion processes. Finally, CO<sub>2</sub> refrigeration systems have been combined with other systems (hybrid systems) to provide air-conditioning, to perform heat recovery, etc..., i. e., to supply all thermal demands of an application using a very efficient combined system (Pardiñas et al., 2018).

In the last years, in parallel with the approval of the F-Gas Regulation in Europe (European Commission, 2014) and the adoption and ratification of the Kigali amendment to the Montreal Protocol (UNEP, 2016), CO<sub>2</sub> refrigeration is in a massive expansion stage, especially in supermarket refrigeration. This sector, which electricity consumption for refrigeration purposes reaches around 45% of its total consumption (International Institute of Refrigeration, 2015), needed a refrigerant that mitigated its large negative contribution to the Greenhouse effect derived from the use of high-GWP refrigerants and high refrigerant leakage rates (from 5 to 23% annually) (Llopis et al., 2015b). The first reason why CO<sub>2</sub> turned out to be the best candidate, was that it combines favourable environmental properties (GWP=1) and high security properties (A1 Ashrae classification). The second reason is that the advance of the technique has allowed implementing CO<sub>2</sub> refrigeration systems competitive or even better than with traditional systems, which increased complexity of course.

Although some upgrades of CO<sub>2</sub> refrigeration systems have been extensively covered in the last decade, the improvements associated with 'subcooling' or 'after-cooling'<sup>1</sup> of CO<sub>2</sub> at the exit of the gas-cooler/condenser have not been analysed globally. Accordingly, the purpose of this review is to join the most recent research in relation to cycles, mechanisms and possibilities to improve the energetic performance of CO<sub>2</sub> refrigeration plants using subcooling at the exit of the gas-cooler/condenser. Revision of the state of the art shows that considering as base line system the CO<sub>2</sub> cycle without improvements, the possibilities to enhance the overall performance reach 12% using internal heat exchangers, 22% using economizers, 25.6% using thermoelectric systems, 21.3% using integrated mechanical subcooling systems and 30.3% using dedicated mechanical subcooling systems (see Table 1 for reference values). Most of the review research is at an initial stage and there is room for improvement in some of the methods.

This review is limited to subcooling systems devoted to CO<sub>2</sub> refrigeration systems and concretely to cycles with subcooling at the exit of the gas-cooler/condenser with the use of heat exchanger. Other options, such as parallel compression technologies (Chesi et al., 2014) are not covered, because they do not directly rely on CO<sub>2</sub> subcooling. Here, we make emphasis on refrigeration systems including an accumulation vessel, being its design is the most appropriate for supermarket application. For these systems, due to the presence of the accumulation vessel, the thermodynamic behaviour of the cycles is independent on the refrigerant charge.

The review is organized as follows: First, in Section 2 the thermodynamic aspects of subcooling in CO<sub>2</sub> refrigeration systems are analysed: cycle modification in subcritical and transcritical conditions, benefits and cost of subcooling and optimization of the systems are addressed. Second, Section 3 is devoted to subcooling mechanisms based on internal methods, i. e., using the CO<sub>2</sub> cycle to provide subcooling: internal heat exchangers, economizers, integrated mechanical subcooling systems and heat storage systems are covered. Third, Section 4 is focused on dedicated subcooling methods, consisting on hybrid systems: dedicated mechanical subcooling, thermoelectric systems and others are reviewed. Finally, Section 5 extracts the main conclusions of the current state-of-the-art and highlights the points and options that require further developments, since as it is concluded there is room for improvement using this approach.

---

<sup>1</sup> Mohammadi, S.M.H. (2018) pointed out that the term 'subcooling' is not suitable to be used, since there is no real subcooling in the supercritical region, and suggested to use the term 'after-cooling'. Authors do agree with the definition of the term. However, most of the research work consider the CO<sub>2</sub> subcooling also in subcritical conditions, where, according to Mohammadi, S.M.H. (2018), the term 'subcooling' would be appropriate. Since most of the research has used the term 'subcooling', authors have followed the same nomenclature. Nonetheless, either 'subcooling' or 'after-cooling' would be equivalent in this manuscript.

## 2. Thermodynamic aspects of CO<sub>2</sub> subcooling

This section is dedicated to discuss the main thermodynamic aspects of CO<sub>2</sub> refrigeration cycles with subcooling. Subsection 2.1 summarizes some CO<sub>2</sub> properties related with the Review; Subsection 2.2 details the basic subcooled cycle and describes the cycle operation principles. Subsection 2.3 establishes the benefits of subcooling, in terms of capacity and COP improvements. Subsection 2.4 discusses about the cost or additional energy input needed to provide the subcooling. And finally, subsection 2.5 details the operating parameters that must be optimized in a subcooled cycle.

### 2.1. Summary of CO<sub>2</sub> properties

CO<sub>2</sub> combines favourable environmental properties (GWP=1), high security properties (A1 Ashrae classification) and excellent thermo-physical properties (Kim et al., 2004), what has made it as preferred refrigerant for centralized commercial purposes, especially for supermarket applications.

CO<sub>2</sub> vapour pressure is high (34.8 bar at 0°C and 16.8 bar at -25°C), its latent heat of phase change (230.9 kJ·kg<sup>-1</sup> at 0°C and 293.3 kJ·kg<sup>-1</sup> at -25°C) combined with its small specific volume (0.0102 kg·m<sup>-3</sup> at 0°C and 0.0228 kg·m<sup>-3</sup> at -25°C) results in volumetric capacity is between 3 to 10 times higher than artificial refrigerants used for centralized commercial systems, which helps reducing dimensions of liquid and vapour lines as well as compressor's (Ma et al., 2013). Transport properties of CO<sub>2</sub>, which play an important role in heat transfer and pressure drop characteristics, are also favourable in contrast with artificial refrigerants, especially its thermal conductivity and viscosity (Kim et al., 2004). However, what makes it a '*special refrigerant*' is its low critical temperature ( $t_c=30.978$  °C) combined with a high critical pressure ( $p_c=73.77$ bar). At environment temperatures higher than its critical temperature, CO<sub>2</sub> cycles perform heat rejection in transcritical conditions (in practice at temperatures higher than 25°C, approximately), where unlike common artificial refrigerants, pressure and temperature are not coupled (Sánchez et al., 2014b). Instead of condensing, CO<sub>2</sub> along the supercritical region experiences a gas-cooling process with a decreasing temperature profile and large glide in the heat rejection process, thus the heat exchanger for energy rejection is known as gas-cooler. Transcritical cycles require optimization of the heat rejection pressure since its energy efficiency is bonded to the pressure at the high side of the cycle. Its optimum value is generally correlated with the environment/gas-cooler exit and evaporation temperatures (Chen and Gu, 2005; Kauf, 1999; Liao et al., 2000). For CO<sub>2</sub> cycles, heat rejection pressures are high (98.5 bar at  $t_o=-0.8$ °C and  $t_{gc,out}=40.4$ °C, 101.2 bar at  $t_o=-10.0$ °C and  $t_{gc,out}=40.2$ °C) and the high pressure rates between heat rejection and the evaporation level cause large exergetic losses that result in reduced energy efficiency values of the corresponding cycles (Cabello et al., 2008).

Reduction of exergetic losses in CO<sub>2</sub> expansion processes has been the '*key*' or the '*challenge*' to enlarge the energy efficiency of CO<sub>2</sub> refrigeration cycles in the last two decades, with great achievements in the development of expanders (Singh and Dasgupta, 2016) and ejectors (Elbel and Lawrence, 2016). This

achievements, already in development, have placed CO<sub>2</sub> cycles at similar energy efficiency level than former refrigerants used for centralized commercial purposes. In addition, in the last decade, subcooling strategies have been also considered to increase the energetic performance of CO<sub>2</sub> cycles, which current state of the art is discussed in this Review.

## 2.2. Cycle with subcooling and operation

CO<sub>2</sub> reference cycle configuration considered for the analysis of subcooling corresponds to the most basic classical layout used for centralized commercial purposes, it being detailed in Figure 1. It consists of a compression system, a gas-cooler/condenser performing heat rejection to the hot sink ( $t_H$ ), a generic subcooling system which function is to subcool the CO<sub>2</sub> absorbing energy along the subcooler at an intermediate temperature ( $t_i < t_H$ ), a back-pressure valve to control the heat rejection pressure and a receiver where the non-in-service refrigerant is stocked. Then, liquid refrigerant is extracted from the vessel and sent to the evaporators where the cycle absorbs the heat load from the cold source ( $t_c$ ). Evaporators are usually controlled by expansion valves maintaining a constant degree of superheat.

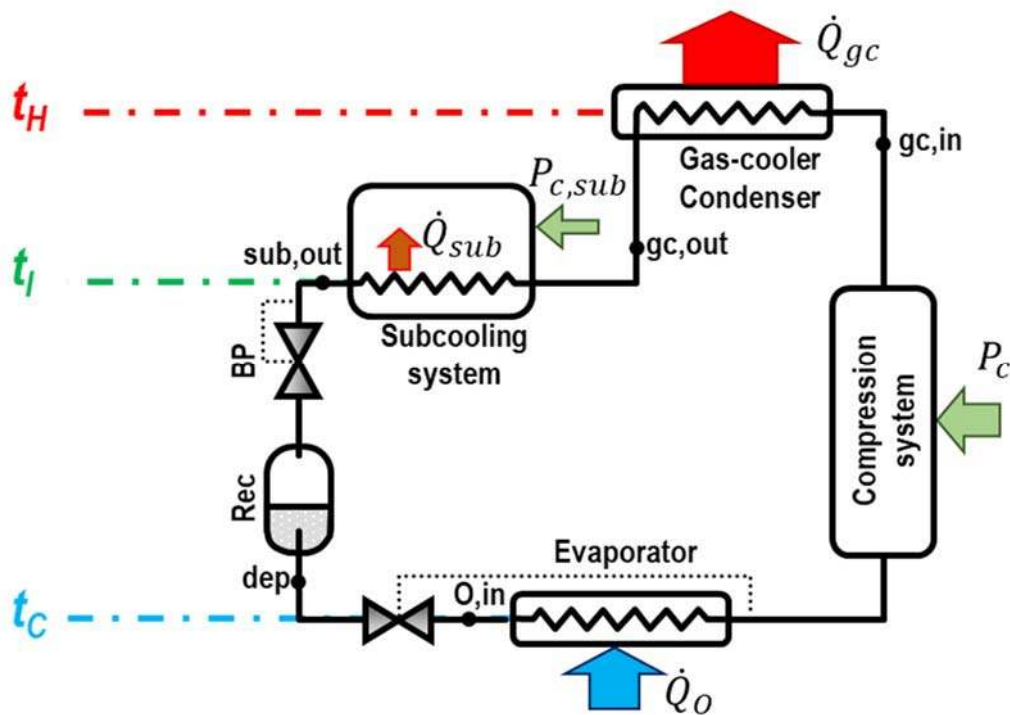


Figure 1. Schematic layout of a CO<sub>2</sub> refrigeration system with double-stage expansion with subcooling system

The low critical temperature of CO<sub>2</sub> ( $t_{crit}=30.978^{\circ}\text{C}$ ) implies that these refrigeration systems run according to two principal modes of operation: at low heat rejection temperature the cycle works in subcritical conditions, where the heat exchanger performs heat rejection through condensation at constant temperature. At high heat rejection temperature, theoretically for heat rejection temperatures above the critical value but in practice for temperatures also below the critical (Sánchez et al., 2014b), the cycle works in supercritical conditions. In this case, the heat exchanger acts as gas-cooler with a decreasing temperature profile through



heat rejection. (Kim et al., 2004). Throughout a year, the refrigeration cycle alternate its operation in subcritical and supercritical conditions, being the analysis needed for both modes of operation.

### **2.2.1. Subcooling in subcritical conditions**

CO<sub>2</sub> subcooling in subcritical conditions can be performed using two types of strategies, extensively analysed by Koeln and Alleyne (2014).

The first one consists of condensing at a forced pressure higher than the minimal that the condenser allows. This situation is represented in Figure 2a with dashed line, with condensing temperature  $t_k^*$  higher than  $t_k$ . In this case, the condenser performs heat rejection at a high temperature and is able to provide a small degree of subcooling by itself (a subcooler device can be used before). This strategy is used in practice for small capacity refrigeration systems for commercial use working with capillary tubes, where the refrigerant mass charge is optimized to obtain a desired subcooling degree in the condenser, as described by Pisano et al. (2015), and thus maximize the energy performance of the system. According to Pottker and Hrnjak (2015), for a single-stage compression cycle with water-cooled-condenser, liquid subcooling below saturation increases the refrigerant effect and the COP of the system, because liquid subcooling reduces the throttling losses in the expansion device. Their simulations for air conditioning systems indicated COP improvements of 8.4% with R-1234yf, 7.0% with R-410A, 5.9% with R-134a and 2.7% with R-717, at condenser and evaporator inlet temperatures of 14°C and 0°C, respectively. The application of this strategy in CO<sub>2</sub> refrigeration plants for centralized commercial purposes (Figure 1) would be possible in practice due to the presence of the back-pressure, which would rise the heat rejection pressure and increase the subcooling degree. However, neither theoretical nor experimental research studies have been found about by the authors in relation to CO<sub>2</sub> systems.

The second strategy corresponds to the usual in centralized commercial systems, which is represented in continuous line in Figure 2. It consist of performing heat rejection at the minimal temperature that the condenser allows ( $t_k$ ), until saturation, and then incorporate a subcooling system to reduce CO<sub>2</sub> liquid temperature. Again, due to availability of the back-pressure, the condensing pressure could be forced to be higher, but the theoretical results of Nebot-Andrés et al. (2017) indicate that the best performing situation is when CO<sub>2</sub> at the exit of the condenser is in saturation. This mode of operation is possible due to the presence of the back-pressure, which must provide a pressure drop ( $\Delta p_{rec}$ ) to guarantee that the vessel is at saturated condition. In this case, as presented in Figure 2a, the subcooling brings about three positive effects in relation to the cycle without subcooling: a pressure reduction in the vessel ( $\Delta p_{rec}$ ), an increase of the specific refrigerating effect ( $\Delta q_o$ ) and a reduction of the vapour quality at the inlet of the evaporator ( $\Delta x_v$ ), which can result in a slight increment of the evaporating level (Qureshi et al., 2013). No negative effects are introduced except of the cost of subcooling, which is discussed in subsection 2.4. Furthermore, as observed in the temperature-entropy diagram in the shaded triangles (Figure 2b), the introduction of the subcooling to the CO<sub>2</sub> cycle also reduces the exergy losses in the throttling processes.

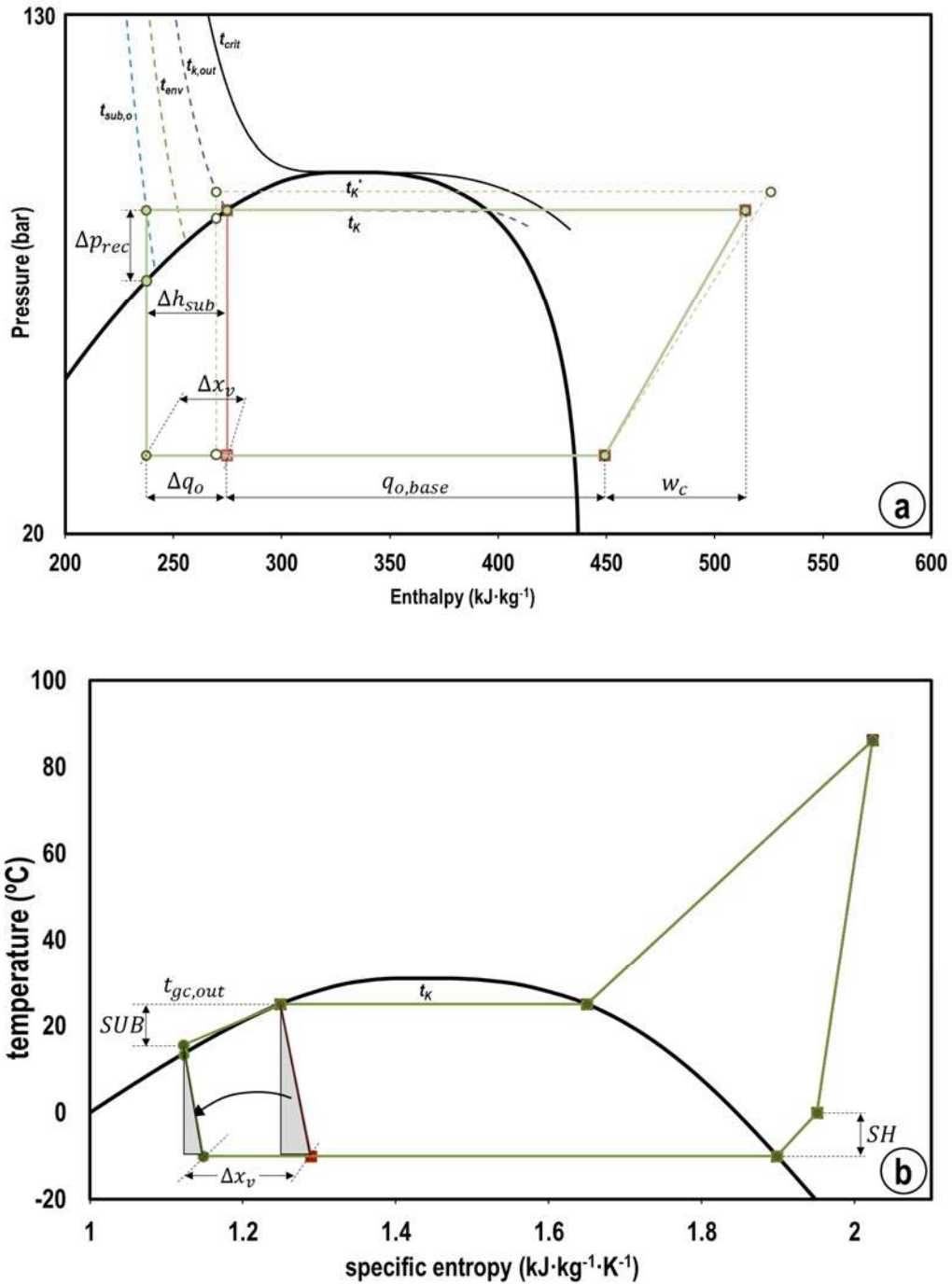


Figure 2. CO<sub>2</sub> cycle (red) and CO<sub>2</sub> with dedicated mechanical subcooling (green) in subcritical conditions.  
a: p-h; b: t-s.  $t_{env}=20^\circ\text{C}$ ,  $t_o=-10^\circ\text{C}$ ,  $\Delta t_{gc}=5\text{K}$ ,  $SH=10\text{K}$ . Adapted from Nebot-Andrés et al. (2017)

### 2.2.2. Subcooling in transcritical conditions

At high heat rejection temperature the refrigeration system operates in transcritical conditions and there is only one possible strategy to subcool the CO<sub>2</sub>, which is represented in Figure 3. It is based on the use of a subcooling system at the exit of the gas-cooler and prior to the back-pressure to provide the desired degree of subcooling. Research discussed in Sections 4 and 5 indicates that subcooling reduces the optimum heat rejection pressure in relation to non-subcooled layouts. Accordingly, the beneficial effects of subcooling are

enhanced in transcritical conditions (Figure 3a), since it allows: a reduction of the optimum heat rejection pressure ( $\Delta p_{gc}$ ), a reduction of the specific compression work in the compressor ( $\Delta w_c$ ), a pressure reduction in the receiver ( $\Delta p_{rec}$ ), an increment of the specific refrigerating effect ( $\Delta q_o$ ) and a reduction of the vapour quality at the inlet of the evaporators ( $\Delta x_v$ ), which can result also in an increment of the evaporating level (Qureshi et al., 2013). Again, the unique drawback is the 'cost of subcooling' or energy input to the subcooling system, which is discussed in 2.3. In addition, according to Figure 3b, it is observed that the subcooling reduces the exergy losses in the expansion devices, and with a larger extend than in subcritical conditions, since the optimum heat rejection pressure is reduced. The subcooling device in transcritical conditions will operate near the critical point, generally crossing the critical isotherm ( $t_{crit}$ ) and sometimes the pseudocritical temperature line ( $t_{ps}$ ), where the isobaric specific heat of CO<sub>2</sub> reaches maximum values (Liao and Zhao, 2002) and CO<sub>2</sub> properties are subjected to large variations, as analysed by Torrella et al. (2011). At high heat rejection temperature, the subcooling system could be subjected to CO<sub>2</sub> properties variations, therefore, it indicates that the design principles of the subcooling heat exchanger should follow the same guidelines as gas-coolers.

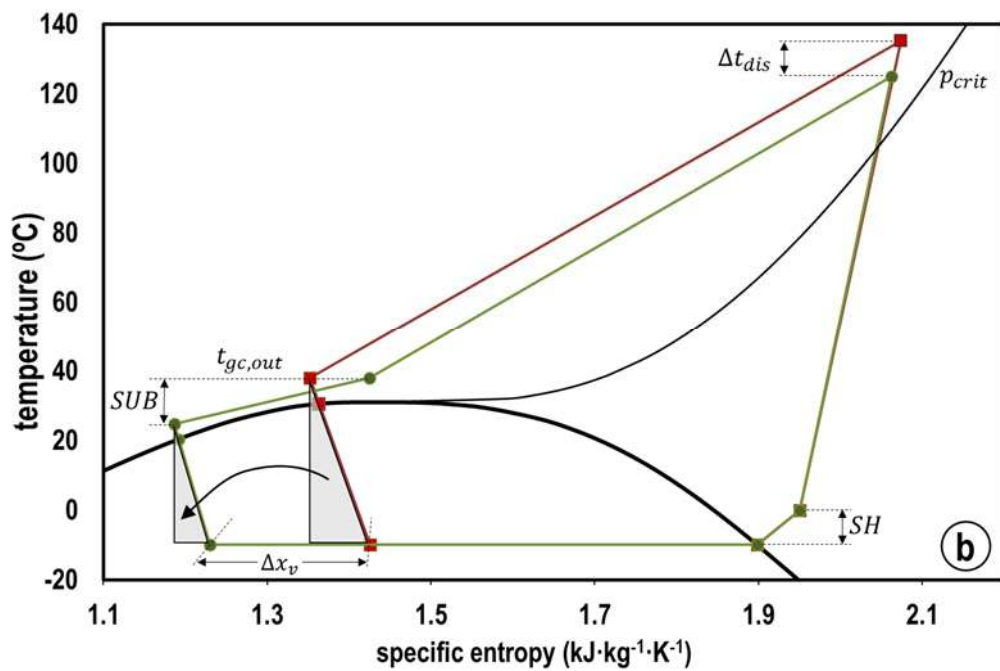
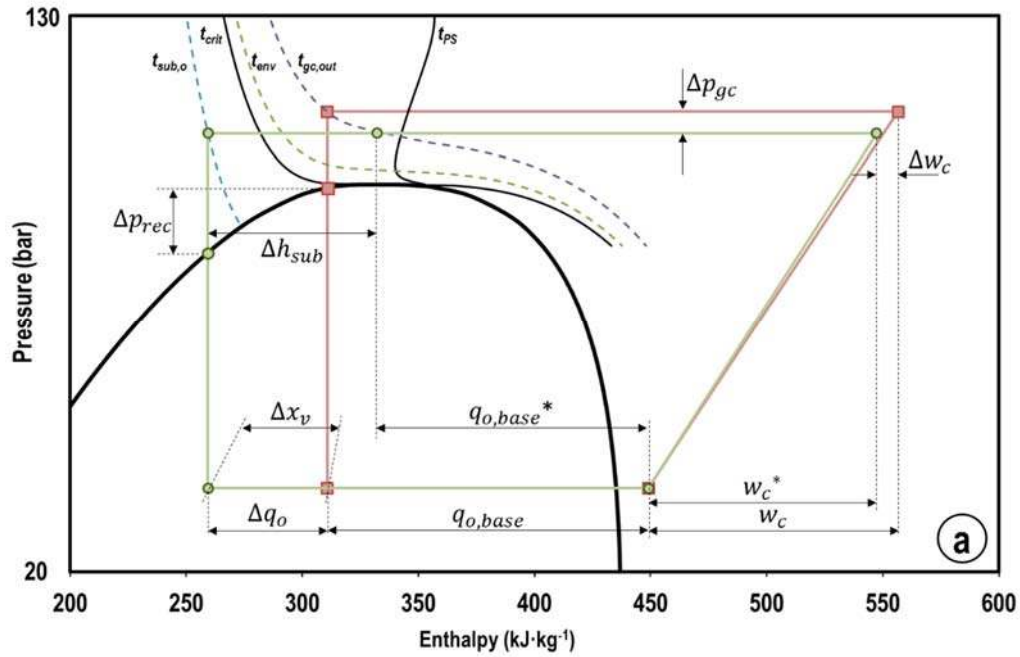


Figure 3. CO<sub>2</sub> cycle (red) and CO<sub>2</sub> with dedicated mechanical subcooling (green) in transcritical conditions.  
a: p-h; b: t-s.  $t_{env}=33^{\circ}\text{C}$ ,  $t_o=-10^{\circ}\text{C}$ ,  $\Delta t_{gc}=5\text{K}$ ,  $SH=10\text{K}$ . Adapted from Nebot-Andrés et al. (2017)

### 2.3. Benefits of subcooling

Subcooling in CO<sub>2</sub> refrigeration systems presents the different advantages or improvements detailed in Section 2.2, nevertheless, a common approach to quantify the practical effects of subcooling is attending to the energy parameters of the refrigeration cycle: capacity and COP.

### 2.3.1. Capacity

Eq. (1) expresses the cooling capacity of the CO<sub>2</sub> refrigeration system with subcooling (Figure 1), which corresponds to the product of refrigerant mass flow rate and the specific refrigerating effect in the evaporator. This term can be expressed as the addition of the capacity of the CO<sub>2</sub> cycle without considering the subcooling ( $\dot{m}_r \cdot q_{o,base}$ ) and the heat extracted by the subcooling device ( $\dot{Q}_{sub}$ ), as expressed by Eq. (2) and (3). The specific refrigerating effect of the cycle without subcooling ( $q_{o,base}$ ), Eq. (4), is the difference between the enthalpy at the exit of the evaporator and at the exit of the gas-cooler/condenser, where "\*" represents enthalpy value at the exit of the gas-cooler/condenser in the new optimum conditions considering the subcooling system, which could be different than of the optimized cycle without subcooling.

$$\dot{Q}_O = \dot{m}_r \cdot q_o = \dot{m}_r \cdot (q_{o,base}^* + \Delta h_{sub}) \quad (1)$$

$$\dot{Q}_O = \dot{m}_r \cdot q_{o,base}^* + \dot{Q}_{sub} \quad (2)$$

$$\dot{Q}_{sub} = \dot{m}_r \cdot \Delta h_{sub} = \dot{m}_r \cdot (h_{gc,out}^* - h_{sub,out}) \quad (3)$$

$$q_{o,base}^* = h_{o,out} - h_{gc,out}^* \quad (4)$$

Table 1 relates the capacity increments achieved by some general subcooling systems, which are expressed in percentage in relation to the reference system used for the evaluation. Torrella et al. (2011) measured up to 12% capacity enhancement by the use of an internal heat exchanger in a single-stage refrigeration plant in relation to the basic layout at high heat rejection temperatures and Llopis et al. (2016a) measured up to 55.7% increase in capacity for a single-stage plant operating with an R-1234yf dedicated mechanical subcooling system at optimum COP conditions. However, the rest of studies were evaluated from a theoretical approach and did not reported the possible capacity increments.

Li et al. (2017) proposed the parameter *RICOSP*, Eq. (5), to quantify the relationship between the increase in capacity of a subcooled vapour compression system ( $\dot{Q}_O - \dot{Q}_{O,no-sub}$ ) to the power or heat extracted by the subcooling device ( $\dot{Q}_{sub}$ ). From a theoretical approach in subcritical cycles, they concluded that the subcooling power cannot be fully transformed into an increase of the cooling output and established the thermodynamic limit of *RICOSP* to 1. At the subcritical conditions shown in Figure 2, neglecting energy losses to the environment, *RICOSP* parameter equals to one since the increment on capacity ( $\Delta q_o$ ) coincides with the enthalpy difference achieved in the subcooler ( $\Delta h_{sub}$ ). In Li et al. (2017) simulations, they calculated a *RICOSP* value of 0.805. However, and also stated by the same authors, if the subcooling modifies the operating conditions of the cycle, as in the case of transcritical conditions (Figure 3), the *RICOSP* can exceed the unit. At the transcritical conditions shown in Figure 3, *RICOSP* exceeds the unit ( $\Delta h_{sub} > \Delta q_o$ ) because the subcooling also increases the refrigerant mass flow rate due to the reduction of optimum heat rejection temperature. For example, Llopis et al. (2016a) measured a *RICOSP* value of

1.19 using an R-1234yf dedicated mechanical subcooling in a single-stage CO<sub>2</sub> refrigerating plant at -10°C of evaporating and 40°C of gas-cooler outlet temperatures at the optimum heat rejection pressure. The use of the subcooling system offered a reduction of the optimum gas-cooler pressure of 5.2 bar, which resulted in an increment of the refrigerant mass flow rate in the CO<sub>2</sub> cycle of 0.5%.

$$RICOSP = \frac{\dot{Q}_O - \dot{Q}_{O,no-sub}}{\dot{Q}_{sub}} \quad (5)$$

Accordingly, it can be deduced that the use of subcooling systems in CO<sub>2</sub> cycles offers highest possibilities than in subcritical conditions, since the subcooling system modifies the operating conditions of the CO<sub>2</sub> cycle towards lower pressures. However, the thermodynamic limits of subcooling in transcritical conditions have not been extensively analysed. Also, expression of RICOSP for CO<sub>2</sub> cycles must be evaluated at the optimum heat rejection pressures.

### 2.3.2. COP

Eq. (6) expresses the COP of a CO<sub>2</sub> refrigeration cycle with subcooling, where:  $\dot{Q}_O$  is the cooling capacity offered by the cycle, Eq. (1);  $P_C$  is the power consumption of the CO<sub>2</sub> compressor; and  $P_{C,sub}$  is the electrical energy input to the subcooling system.

$$COP = \frac{\dot{Q}_O}{P_{C,CO_2} + P_{C,sub}} \quad (6)$$

Defining the COP of the subcooling system as the quotient between the heat extracted by the subcooling device and the energy input to activate the subcooling system, Eq. (7), the overall COP of the subcooled CO<sub>2</sub> refrigeration system can be expressed through an energy balance in the subcooler system as detailed by Eq. (8). In Eq. (8) it is observed that the overall COP depends on the CO<sub>2</sub> enthalpy difference caused by the subcooling system ( $\Delta h_{sub}$ ) and on the COP of the subcooler system ( $COP_{sub}$ ). The subcooling will have positive effect on the COP only if  $\frac{\partial COP}{\partial \Delta h_{sub}}$  results positive. It can be easily demonstrated that the subcooling system will enhance the overall COP if the COP of the subcooling system satisfies Eq. (9) at the operating conditions of the cycle. That is to say that a subcooling system would enhance the performance of a CO<sub>2</sub> cycle as long as  $COP_{sub} = f(t_H, t_I)$  is higher than the  $COP_{sub} = f(t_H, t_C)$  of the CO<sub>2</sub> cycle. In the case of mechanical subcooling systems (subsections 3.3 and 4.1), condition of Eq. (9) is generally satisfied if the subcooling system performs heat rejection to the same hot sink as the CO<sub>2</sub> cycle ( $t_H$ ), because the cold source of the subcooling system ( $t_I$ ) is higher than the cold source of the CO<sub>2</sub> cycle ( $t_C$ ). However, when the subcooling system presents low COP values, such as with the use of thermoelectric devices (subsection 4.2) the improvements are restricted to fulfil Eq. (9) and obtain lower improvements due to the low values of  $COP_{sub}$ . These effects can be observed in the results presented in Table 1. Vapour compression systems used as subcooling systems obtain large improvements in the overall COP because they operate with low temperature difference between the cold source and the heat sink (Llopis et al., 2016a), however, improvements achieved by thermoelectric systems are shorter due to their low COP values (Sarkar, 2013).

$$COP_{sub} = \frac{\dot{Q}_{sub}}{P_{C,sub}} \quad (7)$$

$$COP = \frac{q_{o,base} + \Delta h_{sub}}{w_c^* + \frac{\Delta h_{sub}}{COP_{sub}}} \quad (8)$$

$$COP_{sub} > COP_{CO_2} \quad (9)$$

Accordingly, it can be affirmed that the subcooling systems would offer higher COP increments when higher the COP of the subcooling system is, however, the thermodynamic limits of this improvement have not been extensively analysed.

## 2.4. Energy required by the subcooling system (cost of subcooling)

The cost of subcooling or the additional energy input that the system requires to obtain the subcooling depends on the amount of subcooling to be provided and on the thermodynamic behaviour of the subcooling system. Eq. (10) expresses the total energy input to the system, which considers the energy consumption of the CO<sub>2</sub> cycle and of the subcooling system. Eq. (11) expresses the increment on energy consumption of a subcooled system (\*) in relation to a non-subcooled one.

$$P_C^* = P_{C,CO_2} + P_{C,sub} = \dot{m}_r \cdot w_c + P_{C,sub} \quad (10)$$

$$\Delta P_C = P_C^* - P_C = (\dot{m}_r^* \cdot w_c^* - \dot{m}_r \cdot w_c) + \frac{\dot{Q}_{sub}}{COP_{sub}} \quad (11)$$

Taking as reference the ideal system of Figure 1, if the subcooling is performed in subcritical conditions (Figure 2), the subcooling does not modify the optimum heat rejection pressure and thus the behaviour of condenser and compressor. Correspondingly, the increment on energy input of the subcooled system is the quotient between the heat extracted by the subcooling device and the COP of the subcooling system, Eq. (12). This situation occurs in CO<sub>2</sub> subcritical systems and it is also applicable to conventional refrigerants working in subcritical conditions (Qureshi et al., 2013; Zubair, 1994)

$$\Delta P_C = \frac{\dot{Q}_{sub}}{COP_{sub}} = \dot{m}_r \cdot \frac{\Delta h_{sub}}{COP_{sub}} \quad (12)$$

However, the use of subcooling in transcritical conditions is able to reduce the heat rejection pressure (Figure 3) and thus modify the operating conditions of the compressor. If the heat rejection pressure is lower, the CO<sub>2</sub> refrigerant mass flow rate of the subcooled cycle is higher than the non-subcooled ( $\dot{m}_r^* > \dot{m}_r$ ), but the specific compression work of the subcooled cycle is lower than the non-subcooled ( $w_{comp}^* < w_{comp}$ ), whose trends are opposite. Nonetheless, the experimental results of Llopis et al. (2016a) with a dedicated mechanical subcooling system (DMS) single-stage plant showed that the CO<sub>2</sub> compressor power consumption was reduced when subcooling the cycle, and the results of Bush et al. (2017) with a DMS two-stage plant even resulted in decrements of the total system power consumption. Subsequently, it can be affirmed that the increment on energy consumption due to the subcooling system in transcritical conditions will be lower than the one established in subcritical condition, as expressed by Eq. (13).

$$\Delta P_C < \frac{\dot{Q}_{sub}}{COP_{sub}} = \dot{m}_r \cdot \frac{\Delta h_{sub}}{COP_{sub}} \quad (13)$$



## 2.5. Optimization of subcooling

As mentioned before, subcooling in a CO<sub>2</sub> refrigeration system modifies its optimum operating conditions, especially in transcritical conditions, where the subcooling is able to reduce the optimum high rejection pressure and thus modify the behaviour of the CO<sub>2</sub> compressor. Obviously, it is required for such systems to determine the operating parameters that maximize the COP of the overall system.

COP of the subcooled cycle, Eq. (6), depends on the cooling capacity and on the energy input to the compressor and to the subcooling system. For a fixed operating condition, with defined evaporating level and gas-cooler outlet temperature, the power consumption of the CO<sub>2</sub> compressor only depends on the high rejection pressure, Eq. (14) (Cabello et al., 2008), and the cooling capacity depends on the high rejection pressure as well as on the subcooling, Eq. (15). Referring to the subcooling system, its cold source at  $T_I$  only depends on the subcooling degree, subsequently the energy input to the subcooling system is a function of the subcooling, Eq. (16). Therefore, it can be affirmed that the COP of the whole system is function of the heat rejection pressure and of the subcooling degree, as expressed by Eq. (17). In subcritical conditions the optimum heat rejection pressure is equal to the condensing pressure, as discussed in subsection 2.2, and only the subcooling degree needs to be optimized. However, in transcritical conditions the COP of the plant is bounded to two parameters (Nebot-Andrés et al., 2017) that must be optimized together.

$$P_C = f(p_{gc}) \quad (14)$$

$$\dot{Q}_O = f(p_{gc}, SUB) \quad (15)$$

$$t_I = f(SUB) \rightarrow P_{C,sub} = f(SUB) \quad (16)$$

$$COP = f(p_{gc}, SUB) \quad (17)$$

It is important to highlight that the classical relations to define the optimum heat rejection pressure in CO<sub>2</sub> transcritical cycles (Chen and Gu, 2005; Kauf, 1999; Liao et al., 2000) are not suitable for subcooled cycles, since the optimum condition also depends on the used subcooling system. This is another subject to be investigated concretely for each type of subcooling system.

### 3. Internal methods

This section reviews the methods evaluated to provide the subcooling at the exit of the gas-cooler/condenser internally, i. e. using the cycle itself to cool down CO<sub>2</sub> at the exit of the heat exchanger. Suction-line to liquid-line or internal heat exchangers and their use in different cycle layouts are included in subsection 3.1; the economizer or subcoolers used in two-stage cycles in subsection 3.2; integrated mechanical subcooling systems based on the use of additional compressors in subsection 3.3.; and other internal methods in subsection 3.4.

#### 3.1. Internal Heat Exchanger (IHX)

The use of the IHX was the first subcooling device implemented in the renewed use of CO<sub>2</sub> as refrigerant. In fact, the first researchers who revived the use of CO<sub>2</sub>, Lorentzen and Pettersen (1993), stated that its use in CO<sub>2</sub> refrigeration systems is completely convenient, since it improves COP due to the reduction of the throttling loss from cooling the refrigerant before entering the throttling device, however, they also stated that its use causes strong increments on the compressor discharge temperature.

With artificial refrigerants, the IHX was used as a way to guarantee the right operation of the refrigeration plants, by avoiding liquid entering the compressor and ensuring the presence of liquid at the expansion valves. The IHX presents two opposite effects, an enhancement of the specific cooling capacity and a reduction of the refrigerant mass flow rate due to increased specific suction volume. These opposite effects counteract in artificial refrigerants, where the energy efficiency of the plant could increase or decrease depending on the refrigerant, as studied by Domanski et al. (1994) and Aprea et al. (1999). However, theoretical studies of the IHX in CO<sub>2</sub> transcritical plants (Chen and Gu, 2005; Robinson and Groll, 1998) and the initial experimental studies (Aprea and Maiorino, 2008; Cavallini et al., 2007) clearly demonstrated its beneficial effects in CO<sub>2</sub> systems. In transcritical CO<sub>2</sub> systems, the increase of specific suction volume in the IHX trends to reduce the refrigerant mass flow rate; however, CO<sub>2</sub> subcooling in the IHX in addition to increasing the specific cooling capacity, also reduces the optimal working pressure (see subsection 2.3.1), thus it reduces the compression ratio and tends to increase the refrigerant mass flow rate. In combination, the positive effects dominate over the negative ones, achieving capacity and COP increments, as measured experimentally by the authors reviewed in subsection 3.1.1. Nonetheless, it needs to be mentioned that the use of the IHX subjects the compressor to high discharge temperatures, with temperature increments up to 20K (Torrella et al., 2011), which must be considered in the plant's design.

##### 3.1.1 Classical positions

The IHX or liquid-line-to-suction-line heat exchanger, placed at the exit of the gas-cooler/condenser and at the exit of the evaporator (Figure 5, Layout A), subcools the CO<sub>2</sub> through reheating of the vapours at the exit of the evaporator. In an overall vision, this device increments the specific refrigerating effect in the

evaporator due to the subcooling and increments the compressor suction temperature, as with conventional artificial refrigerants. However, when it is used in transcritical conditions, its use is able to reduce the optimum heat rejection pressure, enhancing the performance of the plant through an increment of the refrigerant mass flow rate and a reduction of the specific compression work in the compressor (section 2.2). Table 2 and Figure 4 collect the experimental COP increments achieved with the use of the IHX in CO<sub>2</sub> refrigeration plants with different typologies. Only specific investigations devoted to the IHX analysis are collected in Table 2.

On the one hand, considering transcritical operation, for environment temperatures higher than 30°C, Cavallini et al. (2005) first simulated an air-to-air double compression with intercooling single-stage throttling cycle with and without IHX quantifying a 7.6% COP improvement due to the IHX, however, in its later experimental verification (Cavallini et al., 2007) they measured 20% COP increment. They argued that the deviation from the theoretical approach was the increased temperature at compressor suction that led to higher heat rejection at the intercooler. Aprea and Maiorino (2008) measured experimentally the IHX effect in an air-to-air single-stage compression two-stage throttling plant for air-conditioning purposes. They measured COP increments from 8.1 to 10.5%. Rigola et al. (2010) evaluated a water-to-water single-throttling plant with an hermetic compressor at -10°C of evaporation, measuring COP increments due to the IHX between 20.5 to 23.2%. This is the largest reported increment, and could be related to the use of a single-stage expansion device or to the use of a hermetic compressor, however, no additional data was reported. Sánchez et al. (2016) tested another water-to-water plant working with a hermetic compressor measuring a maximum COP increment of 6.7% when using the IHX. Finally, Torrella et al. (2011) presented an extensive experimentation of the IHX using a water-to-water double-stage throttling with a single-stage semihermetic compressor at evaporating temperatures from -17 to 0°C. They verified the COP increment, however, the improvements were the lowest among the transcritical tested plants, varying between 3.3 to 9.7% at optimal conditions. All these experimental improvements are summarized in Figure 4.

On the other hand, considering the effect of the IHX in subcritical conditions, Zhang et al. (2011) theoretically predicted a slight COP reduction due to the use of the IHX and advised not to use it in subcritical plants. This COP trend was experimentally verified by Llopis et al. (2015c) in the CO<sub>2</sub> subcritical cycle of a cascade plant with a semihermetic compressor, however, they highlighted that its use at low evaporating levels is needed to guarantee the proper operation of the lubricant oil. Furthermore, in a subsequent investigation (Llopis et al., 2016b) they evaluated the IHX effect in the overall COP of a cascade cycle, concluding that the use of the IHX in the low temperature cycle is also recommended because the overall COP of the cascade was improved up to 3.7%.

Accordingly, from the reported experimental results it is evident that the use of the IHX in the classical layout (exit gas-cooler/exit evaporator) is recommendable for transcritical systems, not for stand-alone subcritical cycles and yes for low-temperature cycles of cascade systems.

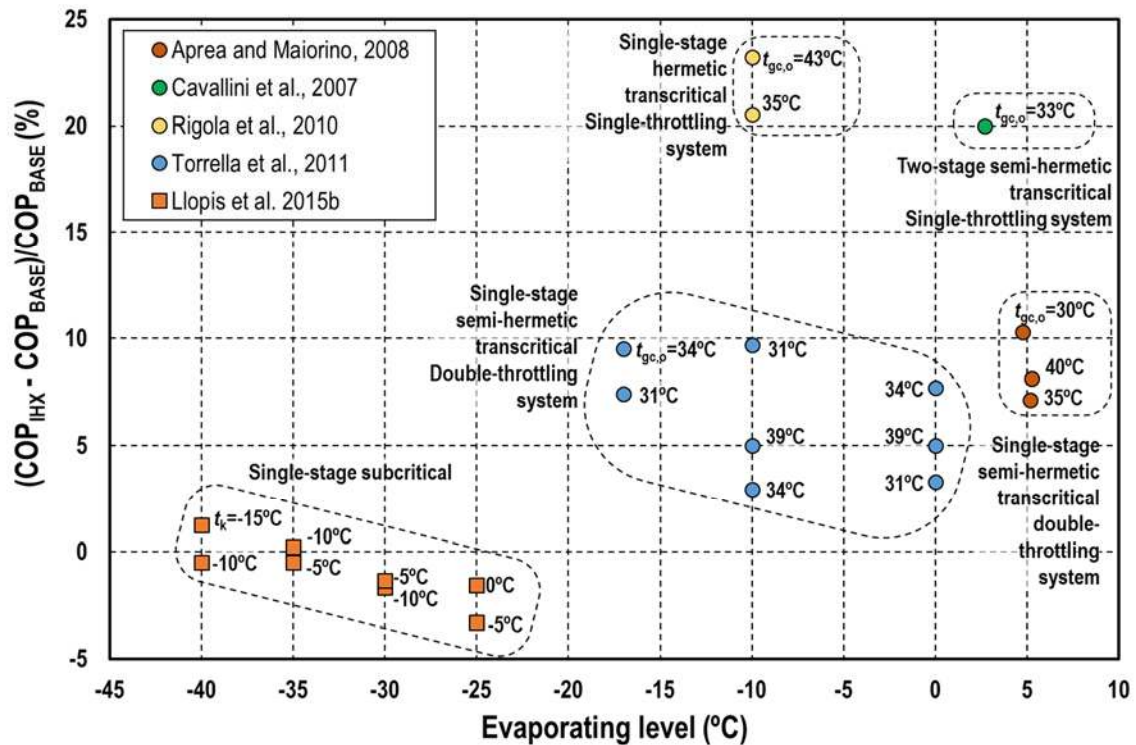
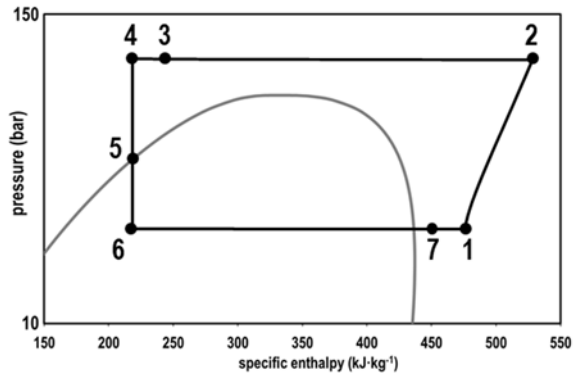
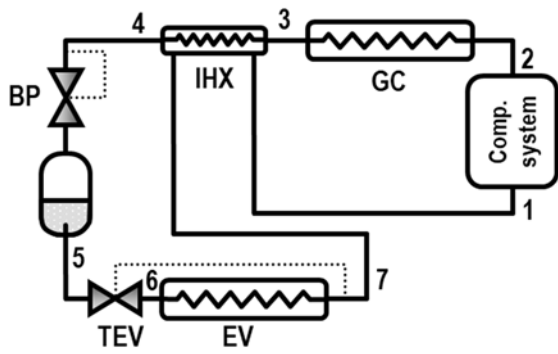


Figure 4. Reported experimental COP improvements in CO<sub>2</sub> refrigeration plants

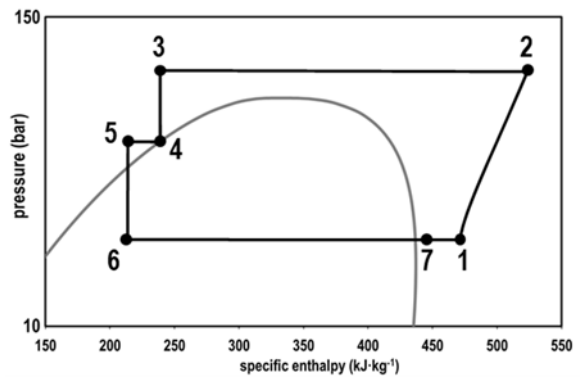
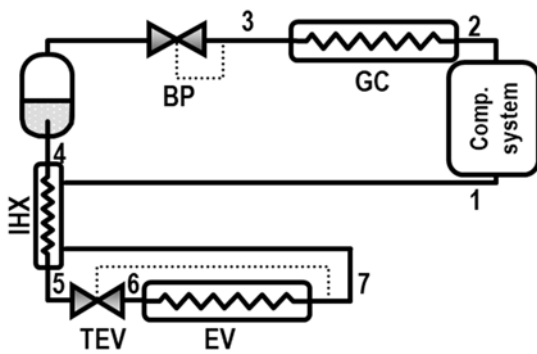
Moreover, additional research was also conducted to evaluate the IHX in different layouts in the refrigeration cycle, as summarized in Table 3. Karampour and Sawalha (2014) theoretically evaluated nine positions of the IHX in a two-stage booster system with heat recovery. After modelling the booster supplying 150kW cooling demand at medium temperature and 50kW at low temperature, they concluded that the IHX provided no significant improvement in terms of refrigeration COP. However, considering simultaneous refrigeration and heat recovery they calculated up to 12% efficiency improvement with IHX at gas-cooler outlet, double IHX at gas-cooler outlet and at the exit of the accumulation tank and double IHX at gas-cooler outlet and at the liquid line to low temperature cabinets, for the booster system with flash gas by-pass. And up to 11% improvement with double IHX at the exit of gas-cooler and at the exit of the accumulation tank, double IHX at gas-cooler outlet and liquid line to low temperature cabinets, double IHX at exit of the accumulation tank and double IHX at exit of accumulation tank and liquid line to low temperature cabinets, for the booster system without flash gas by-pass.

Sánchez et al. (2014a) conducted experimental research with the IHX at three positions in the classical cycle for centralized commercial refrigeration at medium temperature. They evaluated the IHX at the exit of the gas-cooler (Layout A, Figure 5), at the exit of the accumulation receiver (Layout B, Figure 5) and double IHX at the exit of gas-cooler and at the exit of the accumulation receiver (Layout C, Figure 5). They concluded that in any position the IHX resulted positive in terms of COP. However, improvement with Layout B was lower than in the classical position (Layout A) and the Layout C with double IHX provided the largest

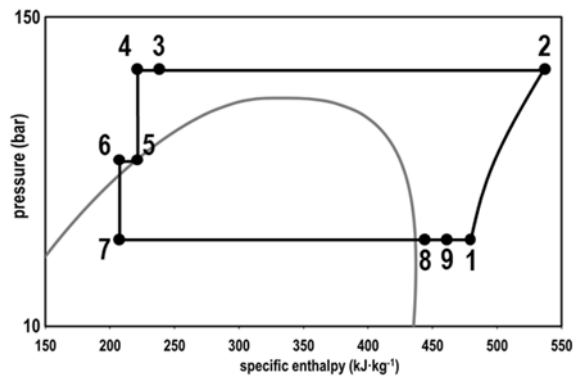
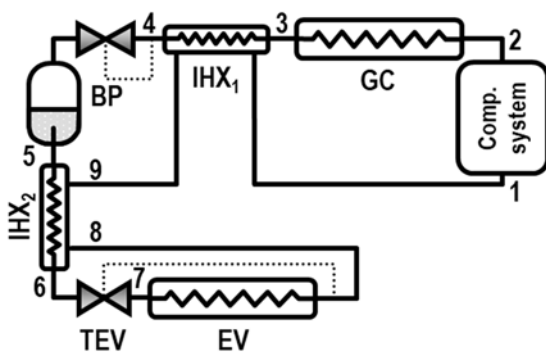
COP increment up to 13%, however, authors advised that the use of two IHX caused increments on the compressor's discharge temperature up to 20K.



IHX at the exit of the gas-cooler/condenser (Layout A)



IHX at the exit of the receiver (Layout B)



Double IHX at the exit of the gas-cooler and at the exit of the receiver (Layout C)

Figure 5. Different IHX layouts

### **3.1.2. Combination of the IHX with ejectors**

Use of IHX has also been considered in CO<sub>2</sub> refrigeration systems using ejectors (**Error! No se encuentra el origen de la referencia.**), whose representative cycle layout is detailed in Figure 6.

First of all, Elbel and Hrnjak (2004) through simulation analysed four different CO<sub>2</sub> air conditioning systems for mobile appliances including a gas ejector and analysed the effect of the IHX on this cycle at 35°C of gas-cooler outlet temperature. They observed that for matching cooling capacities (variable rotational speed of compressor) the system with ejector and without IHX obtained highest COP and reduced optimum heat rejection pressure, however, when the system was analysed under constant rotational speed of the compressor, they observed that the use of the IHX in combination with the ejector obtained the highest COP but reduced the capacity of the system in relation to the system with only ejector. After further analysis, they concluded that the use of the IHX in combination with ejectors with variable displacement compressors was not recommended. Previous theoretical hypothesis were experimentally corroborated by Xu et al. (2011) although in a CO<sub>2</sub> cycle with a two-phase fixed ejector for water heating purposes. They corroborated that the use of the IHX in combination with the ejector weakened the ejector contribution to the system in terms of COP but they observed large increments of the cooling capacity provided by the system with ejector and IHX.

However, experimental results of Nakagawa et al. (2011) with a 2 to 4kW capacity CO<sub>2</sub> refrigeration system with two-phase ejector showed that the IHX was beneficial in combination with the ejector. This different trend can be associated, as stated by the authors, that the improvement achieved by the IHX was larger when higher the heat rejection temperature was and this improvement lowered and even worsened at low temperatures, due to the reduction of pressure recovery in the ejector. In this case, experimental results of Nakagawa et al. (2011) were obtained for gas-cooler outlet temperatures from 42 to 47°C and evaporating temperatures from 0 to 4°C, far away from Xu et al.'s evaluation range (Xu et al., 2011).

Finally, Zhang et al. (2013), using a theoretical approach, extended the analysis of the use of IHX in ejector refrigeration systems. They included in the analysis the ejector isentropic efficiency and extended the simulations to a wide range of evaporating and gas-cooler exit temperatures. They discovered that the use of the IHX is only beneficial in terms of COP for high gas-cooler and evaporating temperatures and for ejector systems with low isentropic efficiency. For systems with ejectors with low isentropic efficiency, the use of the IHX provided highest improvements than the ejector itself, thus its use was not recommendable.

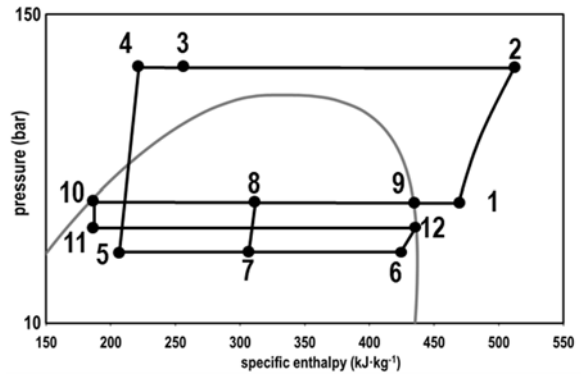
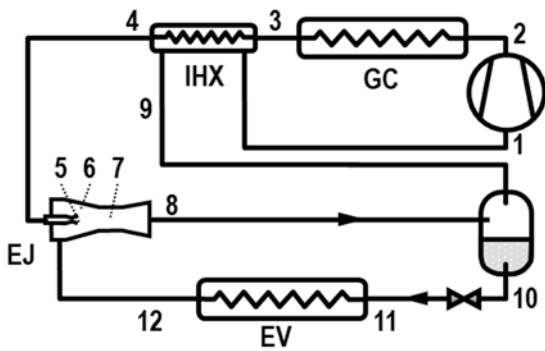


Figure 6. Position of the IHX in CO<sub>2</sub> refrigeration systems with ejector

### 3.1.3. Combination of the IHX with expanders

Use of IHX has scarcely been evaluated in combination with CO<sub>2</sub> refrigeration cycles using expanders to recover energy during the expansion process of the refrigerant, which schematic cycle layout is presented in Figure 7, and the main results summarized in Table 4.

Zhang et al. (2014) and J.Shariatzadeh et al. (2016) using theoretical approaches based on first and second Law of Thermodynamics evaluated the effect of the IHX in the cycle. They concluded that the IHX increases the specific cooling capacity and the compression work, as well as reduced the optimum working pressure. This last effect affected the energy recovered in the expander, making the IHX only beneficial for expanders with low isentropic efficiency at high gas-cooler exit temperatures. They calculated that an ideal expander ( $\eta_{s,exp}=100\%$ ) cycle with IHX presented 12.3 to 16.1% maximum COP reduction in relation to the same cycle without IHX (Zhang et al., 2013).

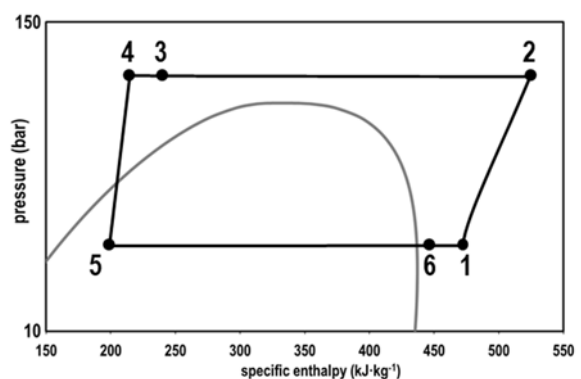
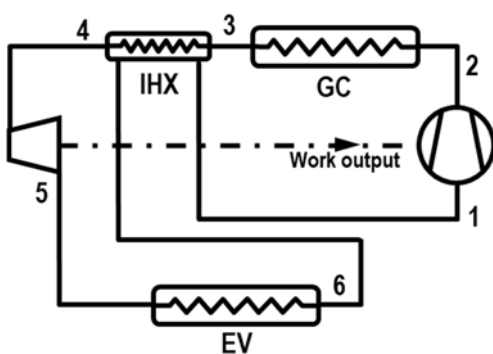


Figure 7. Position of the IHX in CO<sub>2</sub> refrigeration systems with expander

### 3.1.4. IHX with vapour extraction from the intermediate vessel

Finally, the use of the IHX has also been evaluated in combination with vapour extraction from the accumulation vessel. Vapour extraction is performed to increase the specific refrigerating effect in the evaporator through recompression of the extracted vapours. Temperature of extracted vapour is colder than that at the exit of the gas-cooler, thus, it can be used to subcool the main refrigerant steam, as presented in Figure 8 (injection point 'a') in combination with an IHX. Cabello et al. (2012) experimentally evaluated the effect of vapour extraction with expansion from the intermediate vessel and their injection in three positions of a water-to-water CO<sub>2</sub> cycle: a) before the IHX, b) after the IHX and c) at the suction port of the compressor. They concluded that any of the three configurations reached similar increments in capacity and COP reaching maximum values of 9.8 and 7%, respectively, at  $t_{w,o,in}=5^{\circ}\text{C}$  and  $t_{w,gc,in}=34.9^{\circ}\text{C}$ . However, the position providing subcooling (point 'a') allowed the minimum reduction of compressor's discharge temperature among the evaluated configurations. Similar conclusions were obtained theoretically by Karampour and Sawalha (2014) for a booster system.

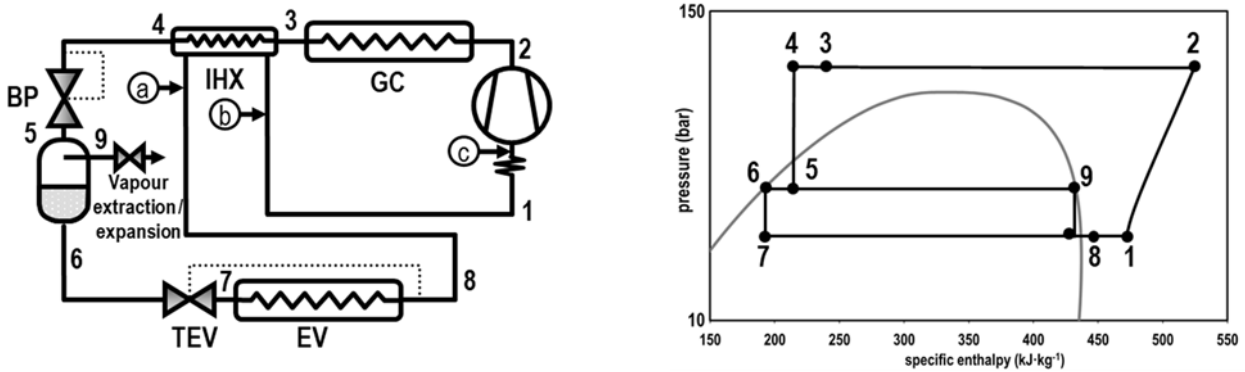


Figure 8. IHX with vapour extraction from the vessel and different injection points



### 3.2. Economizer or subcooler

Use of two-stage cycles brings about the possibility to use specific and more controllable subcooling systems, such as the economized cycle or two-stage cycle with subcooler, which principle scheme is detailed in Figure 9. In this configuration the refrigerant leaving the gas-cooler/condenser is split into two streams. The auxiliary stream is throttled to the intermediate pressure and evaporated inside the economizer or subcooler, allowing to subcool the main steam of refrigerant. As analysed by Torrella et al. (2009), the COP increment that economization allows is dependent on the thermal effectiveness of the subcooler or the closed flash tank separator and the improvement for 100% effectiveness reaches the open flash separator performance at the intermediate pressure.

The first reference found about system was the theoretical study of Cavallini et al. (2005), who denoted it as split cycle and was evaluated for air-conditioning purposes. At an evaporating temperature of 2.7°C and gas-cooler outlet temperature of 33°C they predicted a COP of 3.17 without IHX at the low temperature suction and 3.25 using the IHX. Taking as reference the two-stage cycle with IHX and intercooler, the economized cycle reached a COP improvement of 12.4% and 15.2%, respectively. It must be said that in this study the intermediate pressure considered for the calculation was the geometric mean value of gas-cooler and evaporator temperature, thus not subjected to complete optimization. Then, Cecchinato et al. (2009) theoretically optimized the two-stage split cycle in transcritical conditions and contrasted it to other CO<sub>2</sub> two stage cycles for evaporating levels of 4, -10 and -30°C and external environment temperatures from 25 to 35°C. They concluded that both the open flash tank and split cycle presented the greatest improvement, especially for the heaviest operating conditions (-30 / 35°C).

Later, Wang et al. (2011) theoretically and experimentally analysed a two-stage cycle with closed flash tank separator at the intermediate pressure in contrast to a two-stage cycle with additional gas-cooler at the low-pressure compressor discharge. Through optimization of the intermediate pressure, they verified the higher performance of the closed flash-tank system (10.87% COP increment), but the experimental improvements were lower than those predicted theoretically. Finally, Zhang et al. (2016) theoretically analysed the two-stage cycle with closed flash tank without gas-cooler at the low compression discharge analysing the effect of the use of an expander instead of an expansion valve in the throttling at the gas-cooler exit. They concluded that the two-stage cycle with closed flash tank was best option, it offering higher COP values at low evaporating levels and high gas-cooler outlet temperatures than even the two-stage cycle with intercooler and expander. Despite being a high-performance cycle, no more references, especially experimental, have been found by the authors.

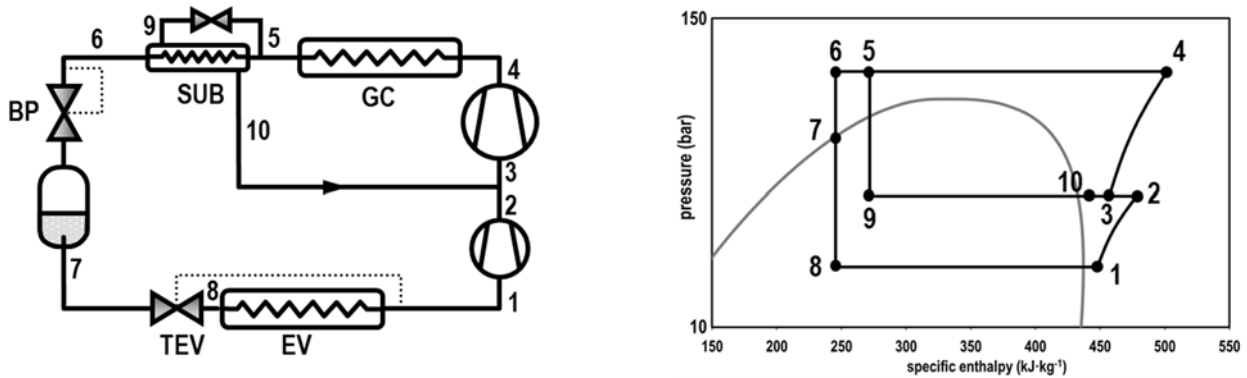


Figure 9. CO<sub>2</sub> two-stage cycle with subcooler or economizer

In a similar way, Fazelpour and Morosuk (2014) theoretically considered the use of the economizer in a single-stage compression system, where vapours at the exit of subcooler were driven directly to compressor suction. The economizer did not affect neither the optimum gas-cooling pressure neither the energy performance of the plant. However, from a second law approach they calculated that the use of the economizer improved by 7% the exergetic efficiency of the cycle, and from an exergoeconomic point of view that the economizer increased the cost of the plant by 4% at an evaporating level of 25°C.

### 3.3. Integrated Mechanical subcooler

Another mechanism to provide large subcooling degrees in the CO<sub>2</sub> at the exit of the gas-cooler/condenser is the integrated mechanical subcooler, whose principle scheme is detailed in Figure 10, and a summary of the conducted research is collected in Table 6. This system splits the stream at the exit of the gas-cooler/condenser and uses the auxiliary one, through throttling in an expansion valve, to subcool CO<sub>2</sub> at the exit of the subcooler. The auxiliary steam is evaporated and compressed by an auxiliary compressor to the high pressure gas-cooler. The advantage of this cycle in contrast to the economized cycle is that the evaporating level in the subcooler could be higher than the intermediate pressure in economized cycles, therefore, the auxiliary compressor could operate with lower compression ratios with higher efficiency. Also, it needs to be mentioned that the extraction of refrigerant for subcooling can be performed at the exit of the gas-cooler (point 4, Figure 10), at the exit of the subcooler (point 5, Figure 10) or at the exit of the vessel (point 5, Figure 10), however no references have been found regarding the two last positions. This cycle can be used as one-level evaporator or as high pressure cycle in booster configurations.

The main advantage of this cycle, in contrast to the split cycle (Figure 9) is that the auxiliary compressor operates with reduced compression ratios and thus with large efficiencies, and in relation to parallel compression systems (Karampour and Sawalha, 2016) is that the displacement of the auxiliary compressor is reduced because it only compresses the evaporated refrigerant instead of vapours from the intermediate vessel. However, at the moment, the operation of the auxiliary compressor and thus the performance of the cycle is limited by the operating restrictions of the compressor, which are a maximum suction pressure

(around 55 bar) and minimum compression ratio (around 1.5). This cycle provides an important increase in cooling capacity and large increments in energy efficiency in relation to basic CO<sub>2</sub> refrigeration cycles.

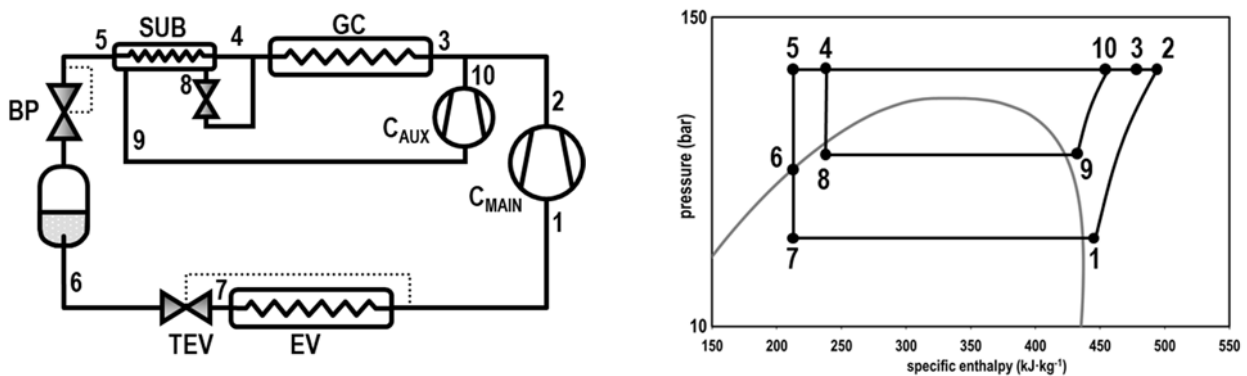


Figure 10. CO<sub>2</sub> cycle with integrated mechanical subcooling

The first reference found to the integrated mechanical subcooling system is the patent of Shapiro (2007). This patent did not refer directly to any refrigerant, therefore it could cover the application in CO<sub>2</sub> systems. Shapiro (2007) reported that the COP of the system was bonded to the evaporating temperature at the subcooler and that the optimum subcooling degree raised at high heat rejection temperature. The first patent covering the integrated mechanical subcooling systems in CO<sub>2</sub> refrigeration cycles is of Kantchev and Lesage (2013), who specifically considered this system as a way to reduce power consumption in compressors and thus enhancing the COP and to increase the cooling capacity of this systems.

Using a theoretical approach, Cecchinato et al. (2009) evaluated 17.3% increase in energy efficiency in relation to a basic single-stage CO<sub>2</sub> cycle at -10°C of evaporating temperature and 30°C of gas-cooler outlet temperature. They concluded that this cycle also overcame the standard double compression cycle, reaching COP increments up to 12%. Their recommendation is to use this system for high evaporating temperature applications. Then, Qureshi and Zubair (2012, 2013) theoretically studied and review the use of the integrated mechanical subcooling system in single-stage refrigeration cycles with artificial refrigerants. They concluded that this auxiliary system enhances the performance of the cycle, however they did not consider CO<sub>2</sub> in their analysis. And finally, Gullo and Cortella (2016) performed an exergoeconomic analysis of the integrated mechanical subcooling system in relation to a standard parallel compressor and a system using a gas ejector for medium temperature applications. They concluded that the integrated system allowed a COP increase 2.8 to 5.5% in relation to the parallel compression system but did not reach the ejector system one. One of the main reasons is that they considered 3K increase in the evaporating level due to the possibility of flooded evaporators. They also highlighted that the integrated solution presented a total investment cost much larger than solutions based on ejector.

Although the possibilities of this subcooling system, no references have been found by the authors in relation to the optimum working conditions (optimum pressures and optimum subcooling degrees) neither validation in experimental systems.

### 3.4. Heat storage systems

Polzot et al. (2016) evaluated the performance of a CO<sub>2</sub> booster system (with and without parallel compressor) when using a water storage system to provide subcooling at the exit of the gas-cooler/condenser for mild climate applications, using the scheme of Figure 11. For the simulations they considered as heat reservoir the fire prevention water tank of a supermarket. During night-time, when the COP of the plant is higher and the cooling demand of the system is low, the water tank is cooled by evaporating liquid CO<sub>2</sub> from the intermediate vessel then it being returned to the vessel. During day-time, the cooled water of the tank is used to subcool the refrigerant at the exit of the gas-cooler/condenser to increase the capacity of the system. Their simulation, for a standard European supermarket of 140kW capacity at MT and 22kW at LT placed in Northern Italy with a 950m<sup>3</sup> water reservoir, resulted in a 2.4% reduction in annual energy consumption of the installation. They also evaluated the possibility to increase the capacity of the reservoir, for double volume the reduction reached 3.5% and for larger volumes the ratio of energy reduction did not increase. Similar conclusions were obtained from a theoretical point of view by Fidorra et al. (2016).

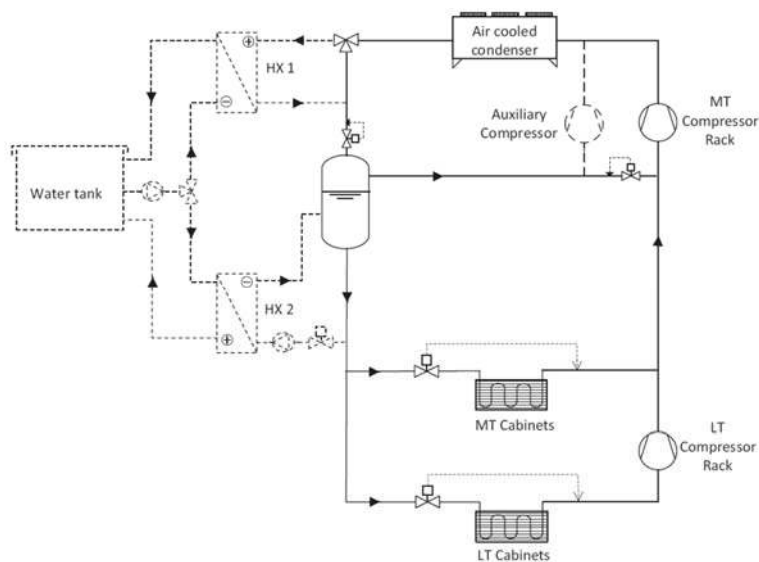


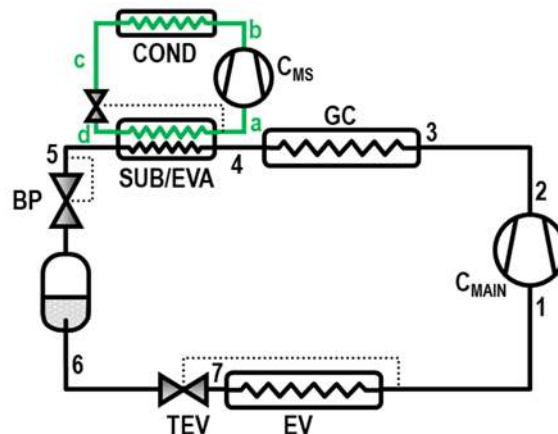
Figure 11. CO<sub>2</sub> booster system with water storage tank (Polzot et al., 2016)

## 4. Dedicated subcooling methods

This section revises the methods evaluated to provide the subcooling at the exit of the gas-cooler/condenser using external or dedicated systems. Dedicated mechanical subcooling systems based on vapour compression technology are analysed in subsection 4.1, thermoelectric subcooling devices in subsection 4.2 and subsection 4.3 collects other scattered external methods.

### 4.1. Dedicated mechanical subcooling (DMS)

Dedicated mechanical subcooling (DMS) or dedicated mechanical aftercooling in CO<sub>2</sub> refrigeration cycles, understood as the use of an additional vapour compression cycle to provide subcooling at the exit of gas-cooler/condenser is one of the recent improvements being investigated by different authors. The DMS, as detailed in Figure 12, consists of an auxiliary vapour compression system especially devoted to subcool the refrigerant at the exit of gas-cooler/condenser. This function can also be performed by air conditioning chillers. Auxiliary and CO<sub>2</sub> cycles perform heat rejection to the same hot source, the CO<sub>2</sub> cycle evaporates at its cool production temperature and the auxiliary one at an intermediate level corresponding to the average temperature in the subcooler minus the temperature difference in the subcooler ( $\Delta T_{sub}$ ), thus this last operates with a reduced temperature lift between the cold source and hot sink, reaching high COP values. The auxiliary cycle generally works with a different refrigerant and is sized to obtain the optimum subcooling degrees, which are dependent on the heat rejection temperature and evaporating level. As analysed theoretically by Llopis et al. (2015a), this system is able to increase the overall COP and the cooling capacity provided by the CO<sub>2</sub> cycle, and its performance is not much dependent on the refrigerant used in the auxiliary cycle. Furthermore, theoretical results of Nebot-Andrés et al. (2017) indicate that this system overcomes the performance of cascade plants for temperature lifts below 28.5K, but considering annual operation its yearly-performance is higher than that of cascades for evaporating levels higher than -15°C, thus covering the medium temperature application range and even the high-pressure cycle of two-stage CO<sub>2</sub> cycles.



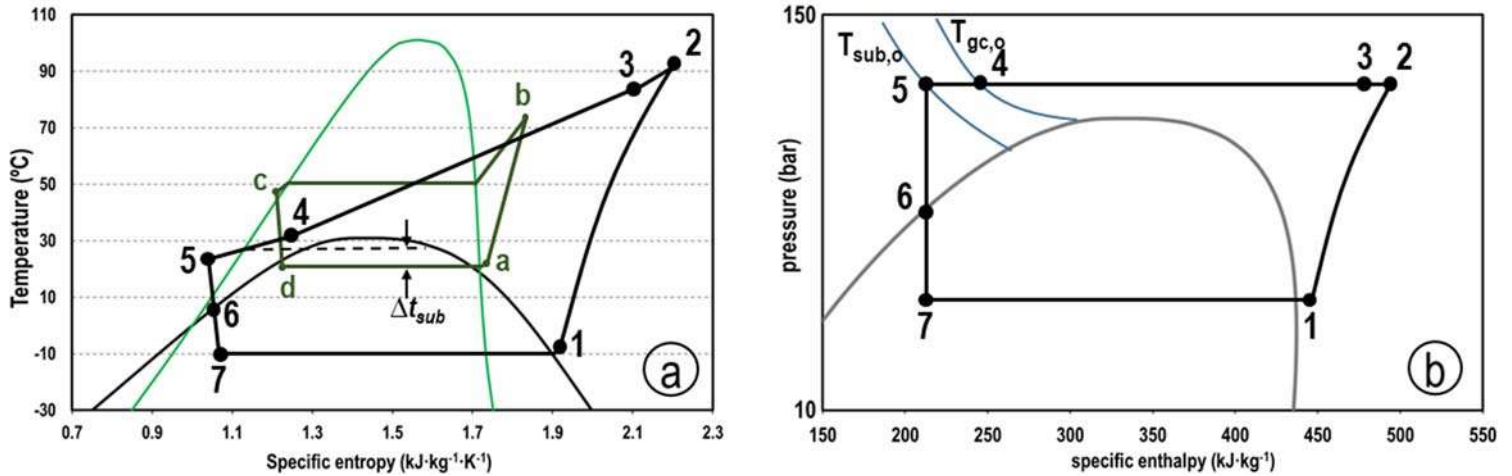


Figure 12. CO<sub>2</sub> refrigeration system with R-134a dedicated mechanical subcooling. (a) T-s diagram. (b) CO<sub>2</sub> p-h diagram.

Table 7 summarises the main theoretical and experimental results in relation to dedicated subcooling methods up to the moment.

The first theoretical studies of DMS systems for CO<sub>2</sub> cycles were performed by Hafner A. and Hemmingsen A. K. (2015), who rated the performance of a R-290 DMS system in a single-stage compression system with flash-tank and IHX at the evaporator exit. In their simulation, they fixed the pressure at the receiver tank at 40bar and considered a DMS with maximum capacity of 30% in relation to the main cycle. They compared the performance of this system with an R-404A direct expansion plant (base line), with the same system without DMS and with a system working with an ejector and parallel compressor. The simulation was extended to different cities and it was observed that the DMS system required between 77 to 97% of the energy input of the base system, and stated that the DMS obtained the highest improvements at high heat rejection temperatures. However, it needs to be mentioned that subcooling optimization was not considered in this study since the capacity of the DMS was limited.

Then, Llopis et al. (2015a) using experimental overall efficiencies of compressors evaluated theoretically the energy improvement of the R-290 DMS in single- and double-stage with intercooling compression cycles at 5, -5 and -30°C of evaporating temperature over a wide range of environment temperatures. Considering as reference system the same cycles without DMS, they predicted maximum COP increments of 20.0% and maximum capacity enhancement of 28.8%, being the improvement of the system higher at higher heat rejection levels and high evaporating temperatures. The largest improvement was achieved for environment temperatures from 25°C on. However, this last work also did not considered optimization of subcooling, it being limited to 7.5K maximum.

In the same line, Gullo et al. (2016) simulated the operation of a booster refrigeration system with R-290 DMS for a typical European supermarket (97kW / -10°C MT, 18kW / -35°C LT) placed in Valencia (Spain) and Athens (Greece). A minimum condensing temperature in the systems was set to avoid low compression

ratios in the high-pressure compressor. They also simulated two designs of the DMS, one that allowed achieving 7°C at the exit of the subcooler and another smaller rated to provide a minimum temperature at the exit of the subcooler of 15°C. In contrast to booster systems with flash gas, they quantified an average COP improvement of 23.2% for the DMS at 15°C and 23.3% for the DMS at 7°C. They emphasized that the DMS at 7°C would operate most of the year at low partial load, and both designs will equally operate at high environment temperature, where the needed capacity in the subcooler decreases. They also evaluated the use of the DMS in booster systems with parallel compressors using R-290 and R-1270 as refrigerants, however those systems did not achieved enough improvement to be recommended.

Dai et al. (2017a) evaluated the impact of the DMS in a single-stage cycle using simplifying assumptions, mainly constant isentropic efficiencies of compressors, for three evaporating levels (5, -5, -15°C) in a wide range of environment temperatures (20-40°C). They focused the study on the evaluation of the COP improvement and high-pressure reduction using different pure refrigerants in the DMS, results were established through optimization of the subcooling degree. They concluded that the optimum subcooling degree is higher as higher the heat rejection and lower the evaporating levels are. Also, they obtained the best improvement with R-717 and the lowest with R-41 as DMS refrigerants, however, it needs to be mentioned that the differences among the different fluids were small.

Next, Purohit et al. (2017) compared different two temperature supermarket refrigeration systems among which there was an R-744 booster solution with a R-290 DMS. Using compressor efficiencies relations obtained from the manufacturer's data, they examined the systems considering temperature and heat load variation along a year for four locations. In relation to the DMS, they concluded that the DMS configuration could be more energetically beneficial than the parallel compression at high outdoor temperature operation. And recently, Dai et al. (2018) from a theoretical point of view evaluated the possibility to use zeotropic refrigerant mixtures as working fluid in the DMS through optimization of high-pressure and subcooling. For an operation of the cycle at -5°C of evaporation and 35°C of environment temperatures, they concluded that COP and optimum high pressure of mixtures with low temperature glide in evaporation are directly correlated with the glide, and that optimized refrigerant mixtures in terms of glide offer a COP improvement and optimum pressure reduction in relation to pure refrigerants. They evaluated different refrigerant mixtures and concluded that mixture R-32/R-1234ze(Z) (55/45 by mass) increased COP by 4.91% and reduced optimum pressure by 11 bar in relation to the use of R-32 as pure refrigerant in the DMS. However, no experimental validation was presented.

A similar approach, was used by She et al. (2014), who studied the classical DMS scheme (Figure 12) but it being activated by the energy recovered by an expander in the CO<sub>2</sub> expansion process. They predicted theoretical COP increments up to 67.76% and recommended R-12 and R-717 as the most beneficial fluids for the auxiliary system.

Using an experimental approach, Nebot-Andrés et al. (2016) presented a preliminary experimental study of the use of an R-1234yf DMS in a single-stage double-throttling refrigeration plant with a 4kW CO<sub>2</sub> and 0.7kW

R-1234yf semihermetic compressors. They evaluated the performance of the plant at nominal speed of compressors at 0°C of evaporation temperature for two gas-cooler exit temperatures (30.2 and 40°C). At the optimum gas-cooler pressures, they measured increments on capacity of 34.9% and 40.7% at 30.2 and 40.0°C respectively and COP increments of 22.8% at 30.2 and 17.3% at 40.0°C. Llopis et al. (2016a) using the same plant extended the experimentation to two evaporating levels (0 and -10°C) and three water inlet temperatures to condenser and gas-cooler (24.0, 30.2 and 40.0°C). The evaluation was also made at constant compressor speeds and only optimization of CO<sub>2</sub> heat rejection pressure was considered. They verified that the optimum heat rejection pressures are reduced by the use of the DMS (up to 8 bar), measured cooling capacity increments at optimum pressure from 23.1 to 55.7% and COP increments from 6.9 to 30.3%. However, this study did not consider optimization of the subcooling degree neither was extended to subcritical conditions. With a small-capacity system working with hermetic compressors, Sánchez et al. (2016) evaluated an R-600a DMS in a CO<sub>2</sub> system working at -10°C of evaporation and two gas-cooler outlet temperatures. They measured increments in capacity from 27.2 to 42.8% and COP increments from 195.1 to 19.3%. Eikevik et al. (2016) simulated, using as reference an experimental prototype, a single-stage compression double-stage throttling refrigeration cycle using a R-290 DMS with scroll compressor. The DMS was activated when the CO<sub>2</sub> high pressure reached 67 bar, thus it did not operate in subcritical conditions. The heat rejection of this prototype was performed by an integrated air cooled CO<sub>2</sub>/R-290 condenser. Their simulations indicated that the best environment temperature to start the DMS was 23.5°C. And they observed high increments on COP and refrigerating capacity over all the tested range, however, they not provided quantification of the improvements. Using data obtained from DMS CO<sub>2</sub> refrigeration systems placed in different warm and hot countries (maximum external temperatures up to 48°C), Mazzola et al. (2016) analysed real effects of the DMS. The systems activated the DMS when the temperature at the exit of the gas-cooler reached 30°C, its operation was restricted to transcritical operation. They compared measurements of energy consumption and maximum discharge temperature as a function of the environment temperature in relation to the same system without DMS. They observed that the DMS allowed 10bar reduction in the discharge pressure and quantified an electric peak reduction between 16 to 40%. After further analysis they concluded that the use of the DMS in those locations reached 25% reduction of energy consumption. And finally, Beshr et al. (2016) and Bush et al. (2017) first simulated and then experimentally validated a prototype of a booster system for supermarket applications with flash tank using an indirect DMS working with R-134a and water-glycol mixture as heat transfer fluid. They evaluated the system under variable speed of the MT compressor and fixed speed of LT and auxiliary compressors for three heat rejection levels, 29, 35 and 39°C. In the experimental verification they observed the theoretical predicted effects, a reduction of the optimum heat rejection pressure (1.9 bar at 29°C, 0.9 bar at 35°C), a large increment of the cooling capacity (+23.7% at 29°C and +37.9% at 35°C) and a big improvement in the overall COP of the system (+33.5% at 29°C and +36.7% at 35°C). Nonetheless, authors did not mention if the system was optimized in terms of subcooling. Recently, Bush et al. (2018) have modelled the system under transient operation.



In relation to subcooler-based CO<sub>2</sub> systems for heat pump applications, the works of (Song and Cao, 2018; Song et al., 2017; Song et al., 2018) have demonstrated that the DMS system is also useful for heating purposes, however, they are not analysed in this manuscript, since it is focused on refrigeration systems.

As it can be seen from the state-of-the-art, the DMS is a system with predicted and evaluated large possibilities of improving the performance of CO<sub>2</sub> refrigeration systems. However, the experimentation phase is not complete, since the experimental evaluation has been only focused on transcritical conditions, in most of the cases, the optimum subcooling degree has not been quantified and the use of zeotropic refrigerant mixtures in the DMS system should be explored.

#### 4.2. Thermoelectric subcooling systems (TSS)

Subcooling at the exit of the gas-cooler, at least with low subcooling degrees, can be also provided using thermoelectric systems, using the simplified scheme of Figure 13. Thermoelectric elements, due to the Peltier effect, generate a temperature difference between both semiconductors that make the element when a DC current is applied to them, therefore they can remove heat from the refrigerant (subcool) and drive it to the environment. One of the advantages of the thermoelectric elements for subcooling is that they operate at a low temperature difference between the cold and hot surfaces (environment temperature and average temperature of CO<sub>2</sub> in the subcooler), where these elements show high COP values. However, the maximum temperature difference at which it can be of profit is when  $COP_{CO_2} < COP_{TSS}$  as discussed in subsection 2.3. The other advantage of the TSS is that it can be activated by the electricity generated by an expander associated with a DC electric generator (Figure 14), thus it being an easy mechanism to take profit of the energy recovered in the expansion process. Table 8 summarizes the most relevant theoretical and experimental works considering TSS in CO<sub>2</sub> refrigeration cycles.

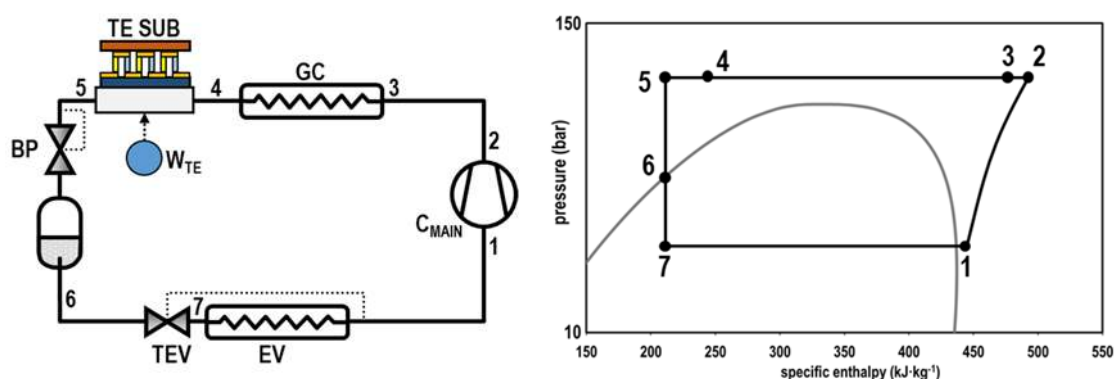


Figure 13. CO<sub>2</sub> refrigeration system with thermoelectric subcooling system

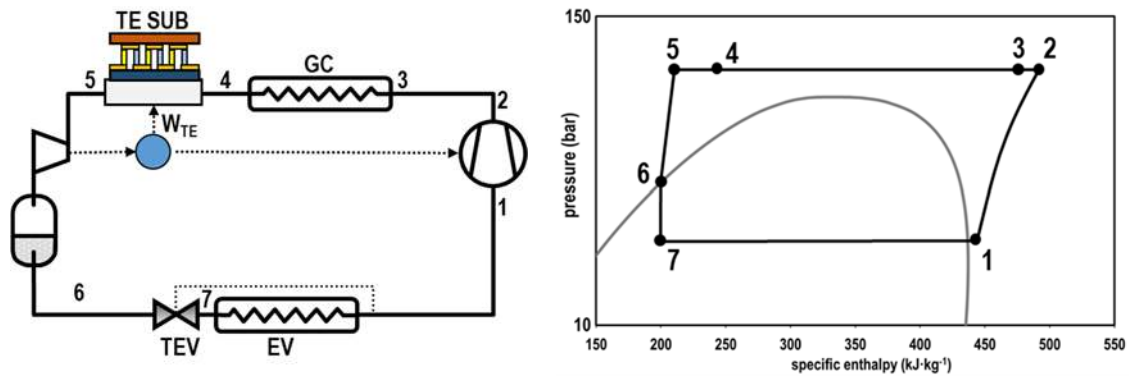


Figure 14. CO<sub>2</sub> refrigeration system with thermoelectric subcooling system and expander

Schoenfield et al. (2008) and Schoenfield et al. (2012) were the first found references testing a TSS in a CO<sub>2</sub> single-stage transcritical refrigeration plant. They used Bismuth-Telluride thermoelectric modules between a microchannel heat exchanger at the cold-side and a single-stage closed thermosyphon working with R22 as heat transfer refrigerant to the environment. They tested the TSS under variable current applied to the thermoelectric elements. In terms of COP, they observed that the highest improvement was achieved for low input current, condition at which the COP<sub>TSS</sub> is highest, however, the COP increment was reduced for higher input currents. Nonetheless, they observed that the capacity of the system also increased with increased input currents. They established two scenarios for comparison with the base line system. When the overall COP value was maximized, they measured 3.3% COP increase jointly with 7.9% increment in capacity, and when the objective function was the capacity, they measured 18.7% increment in capacity jointly with 2.1% reduction in the overall COP. They also theoretically evaluated the possibility to activate the TSS using the energy generated by an expander-electrical generator (Figure 14), reaching the conclusion that it could provide 13% COP enhancement and 11% capacity increment, values higher than those obtained experimentally.

Sarkar (2013) theoretically evaluated a single-stage CO<sub>2</sub> compression system using a TSS to provide subcooling at the exit of the gas-cooler. Using a constant value of the isentropic efficiency of the compressor of 75% and a TSS based on 100 couples bismuth-telluride, he optimized the set performance for gas-cooler exit temperatures from 30 to 50°C and evaporating levels from -15 to 5°C. He highlighted that such a system is bonded to three optimization parameters: high-pressure, subcooling degree and current input to the TSS. He quantified as maximum improvement for an input current of 11A, 25.6% increase in COP and 15.4% discharge pressure reduction. Next, Yazawa et al. (2015) and Yazawa et al. (2016) theoretically evaluated the thermodynamic profit of using an hypothetical TSS to air conditioning systems for data centers. Using thermoelectric elements with a figure-of-merit of 1.5 and 70% isentropic efficiency for the compressor, they predicted 20% COP improvement at a subcooler exit temperature of 12°C for a gas-cooler exit temperature of 40°C. They also presented a cost analysis of the TSS, evaluating a minimum cost of the TSS of 1.5 to 3 \$·W<sup>-1</sup> of cooling capacity, a cost comparable to the cost of a heat exchanger according to the authors. Dai

et al. (2017b) theoretically studied the use of a TSS to a double-compression single-stage CO<sub>2</sub> refrigeration cycle, obtaining similar conclusions to the other authors. In addition, they analysed the possibility of integrating an expander in the system (Figure 14) and the corresponding electric generator to supply the needed DC current to the TSS. They evaluated two possible allocations of the expander, one between the subcooler and the accumulation vessel and the second between the vessel and the evaporator. Their analysis confirmed that the best position was after the subcooler, and for that location the system with TSS and expander predicted a 37.8% COP improvement. And finally, Jamali et al. (2017) gave a step forward and also considered a TSS composed of a two-stage thermoelectric generator recovering energy at the gas-cooler to supply the energy input to another two-stage thermoelectric cooler providing subcooling to the CO<sub>2</sub> at the exit of the gas-cooler. Their simulations at gas-cooler outlet temperatures from 35 to 50°C and evaporating temperatures from -10 to 10°C indicated that, the thermoelectric generator provided only a part of the power needed by the thermoelectric cooler, and for the mentioned cycle the COP improvement reached 18.9% at 5°C of evaporation. However, no experimental validation was presented.

From the literature review about thermoelectric subcooling systems, it is observed that from a theoretical point of view the possibilities of enhancing the performance of the CO<sub>2</sub> refrigeration systems is large, from 3.3 to 37.8%, however the main challenge of this technology is the integration of the thermoelectric elements with the corresponding heat exchangers, where minimization of the thermal resistance is needed to avoid reductions in the operating COP of the thermoelectric elements. Further research, especially with experimental approach is needed.

### **4.3. Other hybrid systems**

Literature reveals some other scattered methods to improve the performance of CO<sub>2</sub> refrigeration systems. Although some of them are not directly focused on achieving subcooling at the exit of the gas-cooler, their principle scheme reveals that it would be possible, and in most of the cases it should be recommended. Arora et al. (2011) combined theoretically a single-stage CO<sub>2</sub> refrigeration plant with a single-stage BrLi-H<sub>2</sub>O absorption plant, activated by heat recovery at gas-cooler, and used to provide additional capacity in the evaporator, at the same temperature level that the refrigeration system. They estimated an increase in capacity from 3.5 to 49.8% and an enhancement of the overall COP between 3.7 to 48.9%. Nonetheless, authors did not investigated the use of the cooling capacity of the absorption system to provide subcooling at the exit of the gas-cooler, method that will also reduce the optimum working pressure and benefit the operation of the compressor. Subcooling by means of an absorption system was analysed by Salajeghe and Ameri (2016). They concluded that the combination reduces the optimum high working pressure, improves the energy utilization factor and reduces the energy consumption in relation to conventional vapour compression systems. Similar conclusions were reached by Mohammadi (2018), who theoretically evaluated different possible combinations of a BrLi-H<sub>2</sub>O absorption with a CO<sub>2</sub> refrigeration systems to

provide 'after-cooling' at the exit of the gas-cooler. However, no experimental studies have been found about the integration of both systems.

Also, Mazzola et al. (2016) analysed experimental data from a CO<sub>2</sub> supermarket installation using groundwater subcooling. The subcooling system was activated at environment temperatures from 25°C, reaching reductions of the optimum high pressure of 15bar at 35°C and 30% energy savings during a year.

Finally, Chen et al. (2017) theoretically analysed and optimized an hybrid CO<sub>2</sub> refrigeration cycle assisted by an ejector cooling system driven by heat rejected by the CO<sub>2</sub> cycle. At evaporation temperatures from 0 to 10°C, the hybrid system allowed 25-30% increase of the overall COP.

## 5. Concluding remarks

In recent years, the use of subcooling methods has been researched and different developments have shown that subcooling of CO<sub>2</sub> at the exit of the gas-cooler/condenser presents numerous advantages in relation to artificial refrigerant cycles, which makes it an improvement to be considered to enhance the performance of such cycles.

This paper comprehensively reviews the work done so far, and the following conclusions have been obtained from the reviewing process:

- CO<sub>2</sub> subcooling, with internal or external methods, enhances the performance of the cycle if the COP of the subcooling system is higher than that reached by the isolated CO<sub>2</sub> cycle. At that situation, benefits of subcooling are a large increase in capacity and an improvement of the overall COP. However, expected improvement in subcritical conditions is lower than in transcritical conditions (high heat rejection temperatures), because in transcritical conditions subcooling reduces the optimum working pressure and maximizes the improvement. Optimization of a CO<sub>2</sub> plant with a subcooling system is bonded to at least two variables, the optimum heat rejection pressure and the degree of subcooling, both bonded to the type of subcooling system.
- About internal methods to provide subcooling: it results obvious that the use of the internal heat exchanger (IHX) is mandatory when CO<sub>2</sub> operates in transcritical conditions, with reported COP increments up to 20% or even more, but this component presents the drawback of increased discharge temperature. The combination of the IHX with expansion energy recovery elements (ejectors and expanders) results negative, since the IHX penalizes those elements. Economization of CO<sub>2</sub> cycles, generally used with double-stage compression systems, showed COP improvements up to 15.2%, the use of integrated mechanical subcooling systems up to 17.5%, and the combination with heat storage systems up to 3.5%.
- Considering external subcooling systems: dedicated mechanical subcooling systems, generally based on the use of an additional vapour compression system with another refrigerant, have been widely investigated, with predicted COP improvements up to 28.8% and up to 67.7% using the

dedicated subcooling system jointly with an expander. However, the theoretical approach seems to be based on conservative assumptions, since the reviewed experimental work reported COP increments nearly up to 40%. It is mentioned that subcooling reduces the size of the CO<sub>2</sub> refrigeration system, however, existing research did not cover it. Thermoelectric subcooling systems are said to enhance the COP of the cycle between 20 to 25.6%, but, its combination with energy recovery systems (expanders or thermoelectric generators) increases this figure up to 37.8%. However, the main drawback of thermoelectric subcooling still relies on the design of the heat exchanger that joins the thermoelectric elements with the subcooler, where thermal resistances have an important role.

Conclusions from actual research reveal that subcooling is a worth method to increase the performance of CO<sub>2</sub> refrigeration systems, however, due to its recent approach the following subjects require further attention:

- Optimum conditions (theoretical or experimental) of integrated and external mechanical methods (subcooling degree and optimum high pressure) have not been extensively investigated. It should be needed to include in the analysis the CO<sub>2</sub> system size reduction and also a thermoeconomic approach would be needed to reach definite conclusions.
- Due to the complexity of the systems, experimental research is needed with integrated mechanical subcooling systems and economized cycles, since the actual research has not reached the improvement limits. Also, the dedicated subcooling systems must be explored from an experimental approach, where the use of refrigerant mixtures in the auxiliary refrigeration cycle could even enhance more the performance. Heat recovery systems integrated with the refrigeration cycle and those based on phase-change materials should be addressed.
- Combination of CO<sub>2</sub> refrigeration cycles with heat recovery systems for subcooling such as absorption systems or adsorption systems is nearly inexistent. The published theoretical works indicate that the combination of these systems would be very positive, however, the experimental evaluation of its combination is a mechanical challenge.
- Recent CO<sub>2</sub> refrigeration cycles rely on the use of ejectors and parallel compression, with great results. However, the introduction of dedicated subcooling systems to them has not been explored extensively. In the case of the ejector, the subcooling system could narrow its operating conditions and help them to simplify its design or regulation.

## Acknowledgements

Authors gratefully acknowledge Ministerio de Economía y Competitividad of Spain (project ENE2014-53760-R.7, grant FPI BES-2015-073612), Jaume I University of Spain (project UJI-B2017-06) and Generalitat Valenciana of Spain (grant ACIF/2017/194) for financing this research work.

## 6. References

- Aprea, C., Ascani, M., De Rossi, F., 1999. A criterion for predicting the possible advantage of adopting a suction/liquid heat exchanger in refrigerating system. *Applied Thermal Engineering* 19, 329-336.
- Aprea, C., Maiorino, A., 2008. An experimental evaluation of the transcritical CO<sub>2</sub> refrigerator performances using an internal heat exchanger. *International Journal of Refrigeration* 31, 1006-1011.
- Arora, A., Singh, N.K., Monga, S., Kumar, O., 2011. Energy and exergy analysis of a combined transcritical CO<sub>2</sub> compression refrigeration and single effect H<sub>2</sub>O-LiBr vapour absorption system. *International Journal of Exergy* 9, 453-471.
- Beshr, M., Bush, J., Aute, V., Radermacher, R., 2016. Steady state testing and modeling of a CO<sub>2</sub> two-stage refrigeration system with mechanical subcooler, *Refrigeration Science and Technology*, pp. 893-900.
- Bush, J., Aute, V., Radermacher, R., 2018. Transient simulation of carbon dioxide booster refrigeration system with mechanical subcooler in demand response operation. *Science and Technology for the Built Environment*, 1-13.
- Bush, J., Beshr, M., Aute, V., Radermacher, R., 2017. Experimental evaluation of transcritical CO<sub>2</sub> refrigeration with mechanical subcooling. *Science and Technology for the Built Environment*, 1-13.
- Cabello, R., Sánchez, D., Llopis, R., Torrella, E., 2008. Experimental evaluation of the energy efficiency of a CO<sub>2</sub> refrigerating plant working in transcritical conditions. *Applied Thermal Engineering* 28, 1596-1604.
- Cabello, R., Sánchez, D., Patiño, J., Llopis, R., Torrella, E., 2012. Experimental analysis of energy performance of modified single-stage CO<sub>2</sub> transcritical vapour compression cycles based on vapour injection in the suction line. *Applied Thermal Engineering* 47, 86-94.
- Cavallini, A., Cecchinato, L., Corradi, M., Fornasieri, E., Zilio, C., 2005. Two-stage transcritical carbon dioxide cycle optimisation: A theoretical and experimental analysis. *International Journal of Refrigeration* 28, 1274-1283.
- Cavallini, A., Corradi, M., Fornasieri, E., 2007. Experimental investigation on the effect of the Internal Heat Exchanger and Intercooler effectiveness of the energy performance of a two-stage transcritical carbon dioxide cycle., in: IIR (Ed.), 22nd International Congress of Refrigeration, Beijing, China.
- Cecchinato, L., Chiarello, M., Corradi, M., Fornasieri, E., Minetto, S., Stringari, P., Zilio, C., 2009. Thermodynamic analysis of different two-stage transcritical carbon dioxide cycles. *International Journal of Refrigeration* 32, 1058-1067.
- Chen, G., Volovyk, O., Zhu, D., Ierin, V., Shestopalov, K., 2017. Theoretical analysis and optimization of a hybrid CO<sub>2</sub> transcritical mechanical compression – ejector cooling cycle. *International Journal of Refrigeration* 74, 86-94.
- Chen, Y., Gu, J., 2005. The optimum high pressure for CO<sub>2</sub> transcritical refrigeration systems with internal heat exchangers. *International Journal of Refrigeration* 28, 1238-1249.
- Chesi, A., Esposito, F., Ferrara, G., Ferrari, L., 2014. Experimental analysis of R744 parallel compression cycle. *Applied Energy* 135, 274-285.
- Dai, B., Liu, S., Li, H., Sun, Z., Song, M., Yang, Q., Ma, Y., 2018. Energetic performance of transcritical CO<sub>2</sub> refrigeration cycles with mechanical subcooling using zeotropic mixture as refrigerant. *Energy* 150, 205-221.
- Dai, B., Liu, S., Sun, Z., Ma, Y., 2017a. Thermodynamic Performance Analysis of CO<sub>2</sub> Transcritical Refrigeration Cycle Assisted with Mechanical Subcooling. *Energy Procedia* 105, 2033-2038.

- Dai, B., Liu, S., Zhu, K., Sun, Z., Ma, Y., 2017b. Thermodynamic performance evaluation of transcritical carbon dioxide refrigeration cycle integrated with thermoelectric subcooler and expander. *Energy* 122, 787-800.
- Domanski, P.A., Didion, D.A., Doyle, J.P., 1994. Evaluation of suction-line/liquid-line heat exchange in the refrigeration cycle. *International Journal of Refrigeration* 17, 487-493.
- Eikevik, T.M., Bertelsen, S., Haugsdal, S., Tolstorebrov, I., Jensen, S., 2016. CO<sub>2</sub> refrigeration system with integrated propan subcooler for supermarkets in warm climate., in: IIR (Ed.), 12th IIR Gustav Lorentzen Natural Working Fluids Conference., Edinburgh, United Kingdom.
- Elbel, S., 2011. Historical and present developments of ejector refrigeration systems with emphasis on transcritical carbon dioxide air-conditioning applications. *International Journal of Refrigeration* 34, 1545-1561.
- Elbel, S., Hrnjak, P., 2004. Effect of Internal Heat Exchanger on Performance of Transcritical CO<sub>2</sub> Systems with Ejector, *International Refrigeration and Air Conditioning Conference*. Paper 708., Purdue University, EEUU.
- Elbel, S., Lawrence, N., 2016. Review of recent developments in advanced ejector technology. *International Journal of Refrigeration* 62, 1-18.
- European Commission, 2014. Regulation (EU) No 517/2014 of the European Parliament and of the Council of 16 April 2014 on fluorinated greenhouse gases and repealing Regulation (EC) No 842/2006.
- Fazelpour, F., Morosuk, T., 2014. Exergoeconomic analysis of carbon dioxide transcritical refrigeration machines. *International Journal of Refrigeration* 38, 128-139.
- Fidorra, N., Minetto, S., Hafner, A., Banasiak, K., Köhler, J., 2016. Analysis of cold thermal energy storage concepts in CO<sub>2</sub> refrigeration systems, *Refrigeration Science and Technology*, pp. 495-502.
- Groll, E.A., Kim, J.-H., 2007. Review Article: Review of Recent Advances toward Transcritical CO<sub>2</sub> Cycle Technology. *HVAC&R Res.* 13, 499-520.
- Gullo, P., Cortella, G., 2016. Comparative Exergoeconomic Analysis of Various Transcritical R744 Commercial Refrigeration Systems, in: Ljubljana, U.o. (Ed.), ECOS 2016 - The 29th International conference on efficiency, cost, optimization, simulation and environmental impact of energy systems., Portoroz, Slovenia.
- Gullo, P., Elmegaard, B., Cortella, G., 2016. Energy and environmental performance assessment of R744 booster supermarket refrigeration systems operating in warm climates. *International Journal of Refrigeration* 64, 61-79.
- Hafner, A., Försterling, S., Banasiak, K., 2014. Multi-ejector concept for R-744 supermarket refrigeration. *International Journal of Refrigeration* 43, 1-13.
- Hafner A., Hemmingsen A. K., 2015. R744 refrigeration technologies for supermarkets in warm climates., in: IIR (Ed.), 24th International Congress of Refrigeration, Yokohama, Japan.
- International Institute of Refrigeration, 2015. 29th Informatory Note on Refrigeration Technologies. The Role of Refrigeration in the Global Economy. IIR, France.
- J.Shariatzadeh, O., Abolhassani, S.S., Rahmani, M., Ziaee Nejad, M., 2016. Comparison of transcritical CO<sub>2</sub> refrigeration cycle with expander and throttling valve including/excluding internal heat exchanger: Exergy and energy points of view. *Applied Thermal Engineering* 93, 779-787.
- Jamali, S., Yari, M., Mohammadkhani, F., 2017. Performance improvement of a transcritical CO<sub>2</sub> refrigeration cycle using two-stage thermoelectric modules in sub-cooler and gas cooler. *International Journal of Refrigeration* 74, 105-115.
- Kantchev, J., Lesage, G., 2013. Mechanical subcooling of transcritical r-744 refrigeration systems with heat pump heat reclaim and floating head pressure. Google Patents.

- Karampour, M., Sawalha, S., 2014. Investigation of using Internal Heat Exchangers in CO<sub>2</sub> Trans-critical Booster System, in: IIF, I.-. (Ed.), 11th IIR Gustav Lorentzen Conference on Natural Refrigerants, Hanzhou, China.
- Karampour, M., Sawalha, S., 2016. Integration of heating and air conditioning into a CO<sub>2</sub> trans-critical booster system with parallel compression. Part I: Evaluation of key operating parameters using field measurements, in: IIR (Ed.), 12th IIR Gustav Lorentzen Natural Working Fluids Conference., Edinburgh, United Kingdom.
- Kauf, F., 1999. Determination of the optimum high pressure for transcritical CO<sub>2</sub>-refrigeration cycles. *International Journal of Thermal Sciences* 38, 325-330.
- Kim, M.H., Pettersen, J., Bullard, C.W., 2004. Fundamental process and system design issues in CO<sub>2</sub> vapor compression systems. *Progress in Energy and Combustion Science* 30, 119-174.
- Koeln, J.P., Alleyne, A.G., 2014. Optimal subcooling in vapor compression systems via extremum seeking control: Theory and experiments. *International Journal of Refrigeration* 43, 14-25.
- Li, Z., Chen, E., Jing, Y., Lv, S., 2017. Thermodynamic relationship of subcooling power and increase of cooling output in vapour compression chiller. *Energy Conversion and Management* 149, 254-262.
- Liao, S.M., Zhao, T.S., 2002. Measurements of heat transfer coefficients from supercritical carbon dioxide flowing in horizontal mini/micro channels. *Journal of Heat Transfer* 124, 413-420.
- Liao, S.M., Zhao, T.S., Jakobsen, A., 2000. A correlation of optimal heat rejection pressures in transcritical carbon dioxide cycles. *Applied Thermal Engineering* 20, 831-841.
- Llopis, R., Cabello, R., Sánchez, D., Torrella, E., 2015a. Energy improvements of CO<sub>2</sub> transcritical refrigeration cycles using dedicated mechanical subcooling. *International Journal of Refrigeration* 55, 129-141.
- Llopis, R., Nebot-Andrés, L., Cabello, R., Sánchez, D., Catalán-Gil, J., 2016a. Experimental evaluation of a CO<sub>2</sub> transcritical refrigeration plant with dedicated mechanical subcooling. *International Journal of Refrigeration* 69, 361-368.
- Llopis, R., Sánchez, D., Sanz-Kock, C., Cabello, R., Torrella, E., 2015b. Energy and environmental comparison of two-stage solutions for commercial refrigeration at low temperature: Fluids and systems. *Applied Energy* 138, 133-142.
- Llopis, R., Sanz-Kock, C., Cabello, R., Sánchez, D., Nebot-Andrés, L., Catalán-Gil, J., 2016b. Effects caused by the internal heat exchanger at the low temperature cycle in a cascade refrigeration plant. *Applied Thermal Engineering* 103, 1077-1086.
- Llopis, R., Sanz-Kock, C., Cabello, R., Sánchez, D., Torrella, E., 2015c. Experimental evaluation of an internal heat exchanger in a CO<sub>2</sub> subcritical refrigeration cycle with gas-cooler. *Applied Thermal Engineering* 80, 31-41.
- Lorentzen, G., 1994. Revival of carbon dioxide as a refrigerant. *International Journal of Refrigeration* 17, 292-301.
- Lorentzen, G., Pettersen, J., 1993. A new, efficient and environmentally benign system for car air-conditioning. *International Journal of Refrigeration* 16, 4-12.
- Ma, Y., Liu, Z., Tian, H., 2013. A review of transcritical carbon dioxide heat pump and refrigeration cycles. *Energy* 55, 156-172.
- Mazzola, D., Sheehan, J., Bortoluzzi, D., Smitt, G., Orlandi, M., 2016. Supermarket application. Effects of sub-cooling on real R744 based trans-critical plants in warm and hot climate. *Data analysis, Refrigeration Science and Technology*, pp. 551-558.
- Mohammadi, S.M.H., 2018. Theoretical investigation on performance improvement of a low-temperature transcritical carbon dioxide compression refrigeration system by means of an absorption chiller after-cooler. *Applied Thermal Engineering* 138, 264-279.



- Nakagawa, M., Marasigan, A.R., Matsukawa, T., 2011. Experimental analysis on the effect of internal heat exchanger in transcritical CO<sub>2</sub> refrigeration cycle with two-phase ejector. *International Journal of Refrigeration* 34, 1577-1586.
- Nebot-Andrés, L., Llopis, R., Sánchez, D., Cabello, R., 2016. Experimental evaluation of a dedicated mechanical subcooling system in a CO<sub>2</sub> transcritical refrigeration cycle, *Refrigeration Science and Technology*, pp. 965-972.
- Nebot-Andrés, L., Llopis, R., Sánchez, D., Catalán-Gil, J., Cabello, R., 2017. CO<sub>2</sub> with Mechanical Subcooling vs. CO<sub>2</sub> Cascade Cycles for Medium Temperature Commercial Refrigeration Applications Thermodynamic Analysis. *Applied Sciences* 7, 955.
- Pardiñas, Á.Á., Hafner, A., Banasiak, K., 2018. Novel integrated CO<sub>2</sub> vapour compression racks for supermarkets. Thermodynamic analysis of possible system configurations and influence of operational conditions. *Applied Thermal Engineering* 131, 1008-1025.
- Peñarrocha, I., Llopis, R., Tárrega, L., Sánchez, D., Cabello, R., 2014. A new approach to optimize the energy efficiency of CO<sub>2</sub> transcritical refrigeration plants. *Applied Thermal Engineering* 67, 137-146.
- Pisano, A., Martínez-Ballester, S., Corberán, J.M., Mauro, A.W., 2015. Optimal design of a light commercial freezer through the analysis of the combined effects of capillary tube diameter and refrigerant charge on the performance. *International Journal of Refrigeration* 52, 1-10.
- Polzot, A., D'Agaro, P., Gullo, P., Cortella, G., 2016. Modelling commercial refrigeration systems coupled with water storage to improve energy efficiency and perform heat recovery. *International Journal of Refrigeration* 69, 313-323.
- Pottker, G., Hrnjak, P., 2015. Effect of the condenser subcooling on the performance of vapor compression systems. *International Journal of Refrigeration* 50, 156-164.
- Purohit, N., Gullo, P., Dasgupta, M.S., 2017. Comparative Assessment of Low-GWP Based Refrigerating Plants Operating in Hot Climates. *Energy Procedia* 109, 138-145.
- Qureshi, B.A., Inam, M., Antar, M.A., Zubair, S.M., 2013. Experimental energetic analysis of a vapor compression refrigeration system with dedicated mechanical sub-cooling. *Applied Energy* 102, 1035-1041.
- Qureshi, B.A., Zubair, S.M., 2012. The impact of fouling on performance of a vapor compression refrigeration system with integrated mechanical sub-cooling system. *Applied Energy* 92, 750-762.
- Qureshi, B.A., Zubair, S.M., 2013. Mechanical sub-cooling vapor compression systems: Current status and future directions. *International Journal of Refrigeration* 36, 2097-2110.
- Rigola, J., Ablanque, N., Pérez-Segarra, C.D., Oliva, A., 2010. Numerical simulation and experimental validation of internal heat exchanger influence on CO<sub>2</sub> trans-critical cycle performance. *International Journal of Refrigeration* 33, 664-674.
- Robinson, D.M., Groll, E.A., 1998. Efficiencies of transcritical CO<sub>2</sub> cycles with and without an expansion turbine: Rendement de cycles transcritiques au CO<sub>2</sub> avec et sans turbine d'expansion. *International Journal of Refrigeration* 21, 577-589.
- Salajeghe, M., Ameri, M., 2016. Effects of further cooling the gas cooler outlet refrigerant by an absorption chiller, on a transcritical CO<sub>2</sub>-compression refrigeration system. *International Journal of Exergy* 21, 110-125.
- Sánchez, D., Catalán-Gil, J., Llopis, R., Nebot-Andrés, L., Cabello, R., Torrella, E., 2016. Improvements in a CO<sub>2</sub> transcritical plant working with two different subcooling systems, *Refrigeration Science and Technology*, pp. 1014-1022.
- Sánchez, D., Patiño, J., Llopis, R., Cabello, R., Torrella, E., Fuentes, F.V., 2014a. New positions for an internal heat exchanger in a CO<sub>2</sub> supercritical refrigeration plant. Experimental analysis and energetic evaluation. *Applied Thermal Engineering* 63, 129-139.

- Sánchez, D., Patiño, J., Sanz-Kock, C., Llopis, R., Cabello, R., Torrella, E., 2014b. Energetic evaluation of a CO<sub>2</sub> refrigeration plant working in supercritical and subcritical conditions. *Applied Thermal Engineering* 66, 227-238.
- Sarkar, J., 2013. Performance optimization of transcritical CO<sub>2</sub> refrigeration cycle with thermoelectric subcooler. *Int. J. Energy Res.* 37, 121-128.
- Schoenfield, J., Hwang, Y., Radermacher, R., 2012. CO<sub>2</sub> transcritical vapor compression cycle with thermoelectric subcooler. *HVAC and R Research* 18, 297-311.
- Schoenfield, J., Muehlbauer, J., Hwang, Y., Radermacher R., 2008. Integration of a thermoelectric subcooler into a carbon dioxide transcritical vapor compression cycle refrigeration system, *International Refrigeration and Air Conditioning Conference*. Paper 903. <http://docs.lib.purdue.edu/iracc/903>.
- Shapiro, D., 2007. Refrigeration system with mechanical subcooling. Google Patents.
- She, X., Yin, Y., Zhang, X., 2014. A proposed subcooling method for vapor compression refrigeration cycle based on expansion power recovery. *International Journal of Refrigeration* 43, 50-61.
- Singh, S., Dasgupta, M.S., 2016. Evaluation of research on CO<sub>2</sub> trans-critical work recovery expander using multi attribute decision making methods. *Renewable and Sustainable Energy Reviews* 59, 119-129.
- Song, Y., Cao, F., 2018. The evaluation of the optimal medium temperature in a space heating used transcritical air-source CO<sub>2</sub> heat pump with an R134a subcooling device. *Energy Conversion and Management* 166, 409-423.
- Song, Y., Li, D., Cao, F., Wang, X., 2017. Investigation of the optimal intermediate water temperature in a combined r134a and transcritical CO<sub>2</sub> heat pump for space heating. *International Journal of Refrigeration* 79, 10-24.
- Song, Y., Ye, Z., Wang, Y., Cao, F., 2018. The experimental verification on the optimal discharge pressure in a subcooler-based transcritical CO<sub>2</sub> system for space heating. *Energy and Buildings* 158, 1442-1449.
- Torrella, E., Llopis, R., Cabello, R., Sánchez, D., 2009. Experimental energetic analysis of the subcooler system in a two-stage refrigeration facility driven by a compound compressor. *HVAC and R Research* 15, 583-596.
- Torrella, E., Sánchez, D., Llopis, R., Cabello, R., 2011. Energetic evaluation of an internal heat exchanger in a CO<sub>2</sub> transcritical refrigeration plant using experimental data. *International Journal of Refrigeration* 34, 40-49.
- UNEP, 2016. Report of the Twenty-Eighth Meeting of the Parties to the Montreal Protocol on Substances that Deplete the Ozone Layer, Kigali, Rwanda.
- Wang, H., Ma, Y., Tian, J., Li, M., 2011. Theoretical analysis and experimental research on transcritical CO<sub>2</sub> two stage compression cycle with two gas coolers (TSCC+TG) and the cycle with intercooler (TSCC+IC). *Energy Conversion and Management* 52, 2819-2828.
- Xu, X.-x., Chen, G.-m., Tang, L.-m., Zhu, Z.-j., Liu, S., 2011. Experimental evaluation of the effect of an internal heat exchanger on a transcritical CO<sub>2</sub> ejector system. *Journal of Zhejiang University-SCIENCE A* 12, 146-153.
- Yazawa, K., Dharkar, S., Kurtulus, O., Groll, E.A., 2015. Optimum design for thermoelectric in a sub-cooled trans-critical CO<sub>2</sub> heat pump for data center cooling, *Annual IEEE Semiconductor Thermal Measurement and Management Symposium*, pp. 19-24.
- Yazawa, K., Liu, Y., Kurtulus, O., Groll, E.A., 2016. Cost optimization of thermoelectric sub-Cooling in air-cooled CO<sub>2</sub> air conditioners, *International Refrigeration and Air Conditioning Conference*. Paper 1626. <http://docs.lib.purdue.edu/iracc/1626>.
- Zhang, F.Z., Jiang, P.X., Lin, Y.S., Zhang, Y.W., 2011. Efficiencies of subcritical and transcritical CO<sub>2</sub> inverse cycles with and without an internal heat exchanger. *Applied Thermal Engineering* 31, 432-438.

Zhang, Z.-y., Ma, Y.-t., Wang, H.-l., Li, M.-x., 2013. Theoretical evaluation on effect of internal heat exchanger in ejector expansion transcritical CO<sub>2</sub> refrigeration cycle. *Applied Thermal Engineering* 50, 932-938.

Zhang, Z., Tian, L., Chen, Y., Tong, L., 2014. Effect of an Internal Heat Exchanger on Performance of the Transcritical Carbon Dioxide Refrigeration Cycle with an Expander. *Entropy* 16, 5919.

Zhang, Z., Wang, H., Tian, L., Huang, C., 2016. Thermodynamic analysis of double-compression flash intercooling transcritical CO<sub>2</sub> refrigeration cycle. *The Journal of Supercritical Fluids* 109, 100-108.

Zubair, S.M., 1994. Thermodynamics of a vapor-compression refrigeration cycle with mechanical subcooling. *Energy* 19, 707-715.

TABLES

Table 1. Improvements of CO<sub>2</sub> refrigeration systems with different subcooling systems. Simple effects.

Subcooling system	Reference system	COP of reference system	$t_o$ (°C)	$t_{gc,out}$ (°C)	Capacity increment in relation to reference system (%)	COP increment in relation to reference system (%)	Type	Reference
Internal heat exchanger	basic cycle to	1.16 ( $t_o=-15.0^\circ\text{C}$ , $t_{gc,out}=33.9^\circ\text{C}$ ) 1.91 ( $t_o=-5.1^\circ\text{C}$ , $t_{gc,out}=31.0^\circ\text{C}$ )	-15 to -5 °C	31 and 34°C	12% max	12% max.	E, O	(Torrella et al., 2011)
Economizer	double-stage cycle with intercooling and	2.62 ( $t_o=2.7^\circ\text{C}$ , $t_{gc,out}=33.0^\circ\text{C}$ ) 2.87 ( $t_o=2.7^\circ\text{C}$ , $t_{gc,out}=22.0^\circ\text{C}$ )	2.7°C	22, 33°C	-	22.1%, 21.0%	T, O	(Cavallini et al., 2005)
Thermoelectric	basic cycle	2.412 ( $t_o=5.0^\circ\text{C}$ , $t_{gc,out}=40.0^\circ\text{C}$ )	-15 to 5°C	30 to 50°C	-	7.0 to 25.6%	T, O	(Sarkar, 2013)
Integrated mechanical subcooler	basic cycle	not provided	-10°C	30 to 42°C	-	20.5 to 21.3%	T, O	(Gullo and Cortella, 2016)
Dedicated mechanical subcooler	basic cycle and	1.32, 1.93, 2.57 ( $t_o=0.0^\circ\text{C}$ , $t_{w,in}=24, 30.2, 40, ^\circ\text{C}$ ) 0.98, 1.44, 1.91 ( $t_o=-10.0^\circ\text{C}$ , $t_{w,in}=24, 30.2, 40, ^\circ\text{C}$ )	0, -10°C	24, 30, 40°C	23.1 to 39.4% ( $t_o=0.0^\circ\text{C}$ ) and 24.2 to 55.7% ( $t_o=-10.0^\circ\text{C}$ )	10.9 to 26.1% ( $t_o=0.0^\circ\text{C}$ ) and 6.9 to 30.3% ( $t_o=-10.0^\circ\text{C}$ )	E	(Llopis et al., 2016a)

T=Theoretical, E= Experimental, O= optimized cycle, Basic cycle: single-stage cycle without IHX

Table 2. Conducted research to quantify the COP improvement due to IHX in the classical position in CO<sub>2</sub> refrigeration plants

Authors	Character	Analysed system	Base system	$t_o$ (°C)	$t_{gc,o} / [t_{env}] /$ $(t_k)$ (°C)	COP measured / predicted	$\Delta$ COP in relation to base system (%)
(Cavallini et al., 2005)	T	Air-to-air double compression with intercooling single-stage throttling with IHX, air-cooled	Same without IHX	2.7	33 [30]	2.82	7.6
(Cavallini et al., 2007)	E	Air-to-air double compression with intercooling single-stage throttling with IHX, air-cooled	Same without IHX	2.7	33 [30]	2.20	20
(Aprea and Maiorino, 2008)	E	Air-to-air single-stage compression two-stage throttling with IHX	Same without IHX	4.5 / 5.25	25 / 40	2.11 / 1.2	8.1 / 10.5
(Cecchinato et al., 2009)	T	Single-throttling single-compression with IHX	Same without IHX	-30 / 4	[30]	1.05 / 3.25	4.8 / 16.5
(Rigola et al., 2010)	E	Water-to-water single-throttling single-compression with IHX	Same without IHX	-10	[35 / 43]	0.875 / 1.175	20.5 / 23.2
(Torrella et al., 2011)	E, O	Water-to-water double-stage throttling single-compression with IHX	Same without IHX	-17 / 0	31 / 39	1.3 / 2.5	3.3 / 9.7
(Llopis et al., 2015c)	E, O	Refrigerant-to-water single-stage throttling single-compression with IHX and desuperheater	Same without IHX	-40 / -25	(-15 / -5)	2.1 / 4.7	-1.7 / 1.22

T=Theoretical, E= Experimental, O= optimized cycle

Table 3. Conducted research to quantify the COP improvement due to IHX in non-classical positions in CO<sub>2</sub> refrigeration systems

Authors	Character	Analysed system	Base system	$t_o / [t_{w,in}] (^{\circ}\text{C})$	$t_{gc,o} / [t_{w,in}] (^{\circ}\text{C})$	COP measured / predicted	max $\Delta\text{COP}$ in relation to base system (%)
Karampour and Sawalha (2014)	T, O	Transcritical booster system with 9 IHX positions. With heat recovery at gas-cooler exit.	Transcritical booster system without IHX. Heat recovery at gas-cooler exit. With and without flash gas by-pass.	$t_{o,MT}=-8^{\circ}\text{C}$ $t_{o,LT}=-12^{\circ}\text{C}$	35	3.3 to 3.75	Booster system with flash gas by-pass: 12% IHX at gc exit (HR), 2-IHX (gc exit, exit accumulation tank), 2-IHX (gc exit, liquid line LT cabinets)  Booster system with flash gas by-pass: 11% 2-IHX (gc exit, exit accumulation tank), 2-IHX (gc exit, liquid line LT cabinets)
Sánchez et al. (2014a)	E, O	Water-to-water single stage cycle with IHX at: a) gc exit, b) exit receiver, c) 2-IHX (gc exit, exit receiver)	Water-to-water single stage cycle without IHX	[5 and 15°C]	[25, 30, 35°C]	(see reference)	a) 10.6% max b) 6.2% max c) 13.0% max

T=Theoretical, E= Experimental, O= optimized cycle

Table 4. Research quantifying the influence of the IHX with ejectors and expanders in CO<sub>2</sub> refrigeration systems

Authors	Character	Analysed system	Base system	Evaporation conditions	Heat rejection conditions	COP measured / predicted	max ΔCOP in relation to base system (%)
Elbel and Hrnjak (2004)	T, O	Air-to-air single-stage cycle with ejector and/or IHX for mobile air conditioning	Air-to-air single-stage cycle without IHX and without ejector	$t_{0,air,in}=35^{\circ}\text{C}$ , 40% RH	$t_{gc,air,in}=35^{\circ}\text{C}$	2.2 at 1500 rpm	+10% at 1500 rpm
						not provided	+26% at variable compressor speed in relation to system with IHX
Xu et al. (2011)	E, O	Water-to-water single-stage cycle with ejector and IHX	Water-to-water single-stage cycle with ejector	$t_{0,w,in}=17^{\circ}\text{C}$	$t_{w,gc,in}=18$ to $26^{\circ}\text{C}$	2.2 to 2.5 (heating COP)	-58 to -62% (heating COP)
Nakagawa et al. (2011)	E	Air-to-water single-stage cycle with ejector and IHX (30, 60cm length)	Air-to-water single-stage cycle with ejector	$t_0=0$ to $4^{\circ}\text{C}$	$t_{gc,out}=42$ to $47^{\circ}\text{C}$	<p>At <math>t_{gc,out}=42^{\circ}\text{C}</math>:</p> <ul style="list-style-type: none"> <li>- 1.4 (<math>t_0=0^{\circ}\text{C}</math>) – 1.73 (<math>t_0=4^{\circ}\text{C}</math>), (Eje. + IHX 30cm)</li> <li>- 1.05 (<math>t_0=0^{\circ}\text{C}</math>) – 1.20 (<math>t_0=4^{\circ}\text{C}</math>), (Eje. + IHX 60cm)</li> </ul> <p>At <math>t_0=0^{\circ}\text{C}</math>:</p> <ul style="list-style-type: none"> <li>- 0.92 (<math>t_{gc,out}=47^{\circ}\text{C}</math>) – 1.54 (<math>t_{gc,out}=42^{\circ}\text{C}</math>), (Eje. + IHX 30cm)</li> <li>- 1.10 (<math>t_{gc,out}=47^{\circ}\text{C}</math>) – 1.70 (<math>t_{gc,out}=42^{\circ}\text{C}</math>), (Eje. + IHX 60cm)</li> </ul>	<p>At <math>t_{gc,out}=42^{\circ}\text{C}</math>:</p> <ul style="list-style-type: none"> <li>- 33% (<math>t_0=0^{\circ}\text{C}</math>) – 44% (<math>t_0=4^{\circ}\text{C}</math>), (Eje. + IHX 30cm)</li> <li>- 52% (<math>t_0=0^{\circ}\text{C}</math>) – 58% (<math>t_0=4^{\circ}\text{C}</math>), (Eje. + IHX 60cm)</li> </ul> <p>At <math>t_0=0^{\circ}\text{C}</math>:</p> <ul style="list-style-type: none"> <li>- 28% (<math>t_{gc,out}=47^{\circ}\text{C}</math>) – 187% (<math>t_{gc,out}=42^{\circ}\text{C}</math>), (Eje. + IHX 30cm)</li> <li>- 42% (<math>t_{gc,out}=47^{\circ}\text{C}</math>) – 243% (<math>t_{gc,out}=42^{\circ}\text{C}</math>), (Eje. + IHX 60cm)</li> </ul>
Zhang et al. (2013)	T, O	Single-stage cycle with ejector and IHX	Single-stage cycle with ejector	$t_0=0, 5, 10^{\circ}\text{C}$	$t_{gc,out}=40, 45, 50^{\circ}\text{C}$	<p>At <math>t_0=5^{\circ}\text{C}</math> and <math>t_{gc,out}=40^{\circ}\text{C}</math>:</p> <ul style="list-style-type: none"> <li>- <math>\eta_{s,eje}=20\%</math>, <math>\epsilon_{IHX}=80\%</math>: 2.52</li> <li>- <math>\eta_{s,eje}=72\%</math>, <math>\epsilon_{IHX}=80\%</math>: 2.85</li> </ul>	<p>At <math>t_0=5^{\circ}\text{C}</math> and <math>t_{gc,out}=40^{\circ}\text{C}</math>:</p> <ul style="list-style-type: none"> <li>- <math>\eta_{s,eje}=20\%</math>, <math>\epsilon_{IHX}=80\%</math>: +3%</li> <li>- <math>\eta_{s,eje}=72\%</math>, <math>\epsilon_{IHX}=80\%</math>: -11%</li> </ul>

Zhang et al. (2014)	T, O	Single-stage cycle with expander ( $\eta_{s,exp}=80\%$ ) and IHX	Single-stage cycle with expander ( $\eta_{s,exp}=80\%$ )	$t_o=0, 5, 10^\circ\text{C}$	$t_{gc,out}=40, 45, 50^\circ\text{C}$	At $t_o=5^\circ\text{C}$ and $t_{gc,out}=40^\circ\text{C}$ : - $\varepsilon_{IHX}=80\%$ : 2.91 - $\varepsilon_{IHX}=60\%$ : 2.95	At $t_o=5^\circ\text{C}$ and $t_{gc,out}=40^\circ\text{C}$ : - $\varepsilon_{IHX}=80\%$ : -10.4% - $\varepsilon_{IHX}=60\%$ : -9.2%
J.Shariatzadeh et al. (2016)	T, O	Single-stage cycle with expander and IHX	Single-stage cycle with expander	$t_o=-25$ to $20^\circ\text{C}$	$t_{gc,out}=30$ to $60^\circ\text{C}$	At $t_o=5^\circ\text{C}$ and $t_{gc,out}=40^\circ\text{C}$ : 2.95	At $t_o=5^\circ\text{C}$ and $t_{gc,out}=40^\circ\text{C}$ : -8.4%

T=Theoretical, E= Experimental, O= optimized cycle



Table 5. Research quantifying the influence of the integrated mechanical subcooler in CO<sub>2</sub> refrigeration systems

Authors	Character	Analysed system	Base system	Evaporation conditions	Heat rejection conditions	COP measured / predicted	max ΔCOP in relation to base system (%)
Cavallini et al. (2005)	T	Two-stage compression system with intercooler and economizer (split-cycle), with and without IHX at evaporator exit	Two-stage compression system with intercooler and without IHX (split-cycle) with and without IHX at evaporator exit	$t_0=2.7^\circ\text{C}$	$t_{gc,out}=33^\circ\text{C}$	<ul style="list-style-type: none"> <li>- Two-stage with intercooler and economizer without IHX at evaporator exit: 3.17</li> <li>- Two-stage with intercooler and economizer without IHX at evaporator exit: 3.25</li> </ul>	<ul style="list-style-type: none"> <li>- +21% (in relation to two-stage with intercooler without IHX)</li> <li>- +15.2% (in relation to two-stage with intercooler and IHX at evaporator exit)</li> </ul>
Cecchinato et al. (2009)	T, O	<ul style="list-style-type: none"> <li>- Two-stage compression system with intercooler and economizer (split-cycle) with IHX at evaporator exit</li> <li>- Two-stage compression system with intercooler and open flash tank with IHX at evaporator exit</li> </ul>	Two-stage compression system with intercooler and IHX at evaporator exit	$t_0=4, -10, -30^\circ\text{C}$	$t_{env}=25$ to $35^\circ\text{C}$	At $t_{env}=30^\circ\text{C}$ : <ul style="list-style-type: none"> <li>- Split-cycle:               <ul style="list-style-type: none"> <li>o <math>t_0=4^\circ\text{C}</math>: 3.70</li> <li>o <math>t_0=-10^\circ\text{C}</math>: 2.57</li> <li>o <math>t_0=-30^\circ\text{C}</math>: 1.72</li> </ul> </li> <li>- Open flash tank:               <ul style="list-style-type: none"> <li>o <math>t_0=4^\circ\text{C}</math>: 3.68</li> <li>o <math>t_0=-10^\circ\text{C}</math>: 2.56</li> <li>o <math>t_0=-30^\circ\text{C}</math>: 1.72</li> </ul> </li> </ul>	At $t_{env}=30^\circ\text{C}$ : <ul style="list-style-type: none"> <li>- Split-cycle:               <ul style="list-style-type: none"> <li>o <math>t_0=4^\circ\text{C}</math>: +9.5%</li> <li>o <math>t_0=-10^\circ\text{C}</math>: +12.7%</li> <li>o <math>t_0=-30^\circ\text{C}</math>: +19.4%</li> </ul> </li> <li>- Open flash tank:               <ul style="list-style-type: none"> <li>o <math>t_0=4^\circ\text{C}</math>: +8.9%</li> <li>o <math>t_0=-10^\circ\text{C}</math>: +12.3%</li> <li>o <math>t_0=-30^\circ\text{C}</math>: +19.4%</li> </ul> </li> </ul>
Wang et al. (2011)	T, E, O	Two-stage compression system with closed flash tank	Two-stage compression system with gas-cooler at the low compression discharge	$t_{w,O,in}= 7$ to $17^\circ\text{C}$ (E)	$t_{gc,out}= 15$ to $25^\circ\text{C}$ (E)	Exact conditions not provided, see reference	Exact increments not provided, see reference
Zhang et al. (2016)	T, O	Two-stage compression cycle	Two-stage compression cycle	$t_0=-10$ to $10^\circ\text{C}$	$t_{gc,out}= 35$ to $50^\circ\text{C}$	At $t_0=5^\circ\text{C}$ and $t_{gc,out}=40^\circ\text{C}$ : 2.76	At $t_0=5^\circ\text{C}$ , $t_{gc,out}=40^\circ\text{C}$ :

		with closed flash tank	with intercooler and throttling valve or expander				<ul style="list-style-type: none"> <li>- +6.5% in relation to cycle with throttling valve:</li> <li>- -15.5% in relation to cycle with expander (<math>\eta_{s,exp}=40\%</math>)</li> <li>- -30.0% in relation to cycle with expander (<math>\eta_{s,exp}=80\%</math>)</li> </ul>
--	--	------------------------	---	--	--	--	---

Table 6. Research quantifying the influence of the integrated mechanical subcooler in CO<sub>2</sub> refrigeration systems

Authors	Character	Analysed system	Base system	Evaporation conditions	Heat rejection conditions	COP measured / predicted	max ΔCOP in relation to base system (%)
Cecchinato et al. (2009)	T, O	Single-stage cycle with integrated mechanical subcooler	Single-stage cycle without IHX	$t_0=4, -10, -30^{\circ}\text{C}$	$t_{env}=25$ to $35^{\circ}\text{C}$	At $t_{env}=30^{\circ}\text{C}$ : <ul style="list-style-type: none"> <li>○ <math>t_0=4^{\circ}\text{C}</math>: 3.72</li> <li>○ <math>t_0=-10^{\circ}\text{C}</math>: 2.37</li> <li>○ <math>t_0=-30^{\circ}\text{C}</math>: 1.33</li> </ul>	At $t_{env}=30^{\circ}\text{C}$ : <ul style="list-style-type: none"> <li>○ <math>t_0=4^{\circ}\text{C}</math>: +16.3%</li> <li>○ <math>t_0=-10^{\circ}\text{C}</math>: +17.3%</li> <li>○ <math>t_0=-30^{\circ}\text{C}</math>: +25.5%</li> </ul>
Gullo and Cortella (2016)	T, O	Single-stage cycle with integrated mechanical subcooler	Single-stage cycle with parallel compressor	$t_0=-10^{\circ}\text{C}$	$t_{env}=30$ to $42^{\circ}\text{C}$	Not provided	<ul style="list-style-type: none"> <li>○ <math>t_{env}=30^{\circ}\text{C}</math>: +2.8%</li> <li>○ <math>t_{env}=34^{\circ}\text{C}</math>: +4.4%</li> <li>○ <math>t_{env}=38^{\circ}\text{C}</math>: +4.5%</li> <li>○ <math>t_{env}=42^{\circ}\text{C}</math>: +5.5%</li> </ul>

T=Theoretical, E= Experimental, O= optimized cycle

Table 7. Research quantifying the influence of the dedicated mechanical subcooling system in CO<sub>2</sub> refrigeration cycles

Authors	Character	Analysed system	Base system	Evaporation conditions	Heat rejection conditions	COP measured / predicted	max ΔCOP in relation to base system (%)
Hafner A. and Hemmingsson A. K. (2015)	T	R-290 DMS single-stage compression system with flash-tank and IHX. (Capacity of DMS limited to 30% of CO <sub>2</sub> cycle)	R-404A direct expansion plant and Standard CO <sub>2</sub> booster	Commercial refrigeration at medium temperature (value not provided)	$t_{env}=-15$ to 43°C	At $t_{env}=27.5^\circ\text{C}$ : 3.0	<ul style="list-style-type: none"> <li>- +15.4% in relation to CO<sub>2</sub> standard booster.</li> <li>- +6.0% in relation to R-404A system</li> </ul>
Llopis et al. (2015a)	T	R-290 DMS single-stage and double-stage cycles (SUB limited to 7.5K)	CO <sub>2</sub> single-stage and double-stage cycles without subcooling	$t_0=-30, -5, 5^\circ\text{C}$	$t_{env}=20$ to 35°C	At $t_{env}=30^\circ\text{C}$ , SUB=7.5K: <ul style="list-style-type: none"> <li>o <math>t_0=-30^\circ\text{C}</math>: 1.36</li> <li>o <math>t_0=-5^\circ\text{C}</math>: 2.38</li> <li>o <math>t_0=5^\circ\text{C}</math>: 3.48</li> </ul>	At $t_{env}=30^\circ\text{C}$ , SUB=7.5K: <ul style="list-style-type: none"> <li>o <math>t_0=-30^\circ\text{C}</math>: +18.4%</li> <li>o <math>t_0=-5^\circ\text{C}</math>: +17.9%</li> <li>o <math>t_0=5^\circ\text{C}</math>: +12.3%</li> </ul>
Gullo et al. (2016)	T	R-290 DMS CO <sub>2</sub> booster system with flash gas valve for supermarket applications (SUB <sub>max</sub> = 7 and 15K)	Conventional CO <sub>2</sub> booster system with flash gas valve for supermarket applications	MT: $t_0=-10^\circ\text{C}$ , $Q_0=97\text{kW}$  LT: $t_0=-35^\circ\text{C}$ , $Q_0=18\text{kW}$	$t_{env}=0$ to 40°C	At $t_{env}=30^\circ\text{C}$ , 1.46	At $t_{env}=30^\circ\text{C}$ , +32.7%
Dai et al. (2017a)	T, O	R-152a DMS single-stage cycle		$t_0=-30, -5, 5^\circ\text{C}$	$t_{env}=20$ to 40°C	At $t_0=0^\circ\text{C}$ , $t_{env}=30^\circ\text{C}$ : 2.85	At $t_0=0^\circ\text{C}$ , $t_{env}=30^\circ\text{C}$ : +25.3%
Purohit et al. (2017)	T, O	R-290 DMS CO <sub>2</sub> booster system with flash gas valve for supermarket applications	CO <sub>2</sub> booster system with parallel compression for supermarket applications	MT: $t_0=-10^\circ\text{C}$ , $Q_0=120\text{kW}$  LT: $t_0=-35^\circ\text{C}$ , $Q_0=25\text{kW}$	$t_{env}=0$ to 45°C	At $t_{env}=30^\circ\text{C}$ , 1.9	At $t_{env}=30^\circ\text{C}$ , 4.4%

Dai et al. (2018)	T, O	DMS with zeotropic mixtures with CO <sub>2</sub> single-stage cycle and single throttling process	CO <sub>2</sub> single-stage cycle and single throttling process	$t_o = -40$ to $10^\circ\text{C}$	$t_{env} = 20$ to $40^\circ\text{C}$	At $t_o = -5^\circ\text{C}$ , $t_{env} = 35^\circ\text{C}$ , for R32/R1234ze(Z) at 60/40 by mass: 2.303	At $t_o = -5^\circ\text{C}$ , $t_{env} = 35^\circ\text{C}$ , for R32/R1234ze(Z) at 60/40 by mass: 38.1%
Nebot-Andrés et al. (2016)	E	R1234yf DMS CO <sub>2</sub> single-stage plant with two-stage throttling	CO <sub>2</sub> single-stage plant with two-stage throttling without IHX	$t_o = 0^\circ\text{C}$	$t_{w,gc,in} = 30.2$ and $40^\circ\text{C}$	<ul style="list-style-type: none"> <li>At <math>t_{w,gc,in} = 30.2^\circ\text{C}</math>: 2.37</li> <li>At <math>t_{w,gc,in} = 40.0^\circ\text{C}</math>: 1.68</li> </ul>	<ul style="list-style-type: none"> <li>At <math>t_{w,gc,in} = 30.2^\circ\text{C}</math>: 22.8%</li> <li>At <math>t_{w,gc,in} = 40.0^\circ\text{C}</math>: 27.3%</li> </ul>
Llopis et al. (2016a)	E, O	R1234yf DMS CO <sub>2</sub> single-stage plant with two-stage throttling	CO <sub>2</sub> single-stage plant with two-stage throttling without IHX	$t_o = -10, 0^\circ\text{C}$	$t_{w,gc,in} = 20.0, 30.2$ and $40.0^\circ\text{C}$	<ul style="list-style-type: none"> <li>At <math>t_o = 0^\circ\text{C}</math>: 2.85, 2.35, 1.67 at <math>t_{w,gc,in} = 24.0, 30.2, 40.0^\circ\text{C}</math> resp.</li> <li>At <math>t_o = -10^\circ\text{C}</math>: 2.04, 1.78, 1.27 at <math>t_{w,gc,in} = 24.0, 30.2, 40.0^\circ\text{C}</math> resp.</li> </ul>	<ul style="list-style-type: none"> <li>At <math>t_o = 0^\circ\text{C}</math>: 10.9, 22.1, 26.1% at <math>t_{w,gc,in} = 24.0, 30.2, 40.0^\circ\text{C}</math> resp.</li> <li>At <math>t_o = -10^\circ\text{C}</math>: 6.9, 24.1, 30.3% at <math>t_{w,gc,in} = 24.0, 30.2, 40.0^\circ\text{C}</math> resp.</li> </ul>
Sánchez et al. (2016)	E, O	R600a DMS CO <sub>2</sub> single-stage plant with two-stage throttling with hermetic compressors	CO <sub>2</sub> single-stage plant with two-stage throttling with hermetic compressors, with and without IHX	$t_o = -10^\circ\text{C}$	$t_{w,gc,in} = 30$ and $35^\circ\text{C}$	At $t_o = -10^\circ\text{C}$ and $t_{w,gc,in} = 35^\circ\text{C}$ : 1.62	At $t_o = -10^\circ\text{C}$ and $t_{w,gc,in} = 35^\circ\text{C}$ : <ul style="list-style-type: none"> <li>20.0% base cycle without IHX</li> <li>9.5% base cycle with IHX</li> </ul>
Beshr et al. (2016) and Bush et al. (2017)	E	R134a DMS CO <sub>2</sub> booster system with open flash tank for supermarket application with two evaporating levels	CO <sub>2</sub> booster system with open flash tank for supermarket application with two evaporating levels	<i>not provided</i>	$t_{env} = 8$ to $40^\circ\text{C}$	At $t_{env} = 29^\circ\text{C}$ : 1.99 (combined COP)	At $t_{env} = 29^\circ\text{C}$ : 33.5%

T=Theoretical, E= Experimental, O= optimized cycle

Table 8. Research quantifying the influence of the thermoelectric subcooling system in CO<sub>2</sub> refrigeration cycles

Authors	Character	Analysed system	Base system	Evaporation conditions	Heat rejection conditions	COP measured / predicted	max ΔCOP in relation to base system (%)
Schoenfield et al. (2008) Schoenfield et al. (2012)	E, O	Single-stage CO <sub>2</sub> cycle with single expansion, with thermoelectric subcooler with R22 thermosyphon	Single-stage CO <sub>2</sub> cycle with single expansion without IHX	$t_o=7.2^{\circ}\text{C}$	$t_{env}=35^{\circ}\text{C}$	2.51	<ul style="list-style-type: none"> <li>+3.3% at maximum COP</li> <li>-2.1% at maximum capacity</li> </ul>
Sarkar (2013)	T, O	Single-stage CO <sub>2</sub> cycle with single expansion, with thermoelectric subcooler	Single-stage CO <sub>2</sub> cycle with single expansion without IHX	$t_o=-15, -5 \text{ and } 5^{\circ}\text{C}$	$t_{gc,out}=30 \text{ to } 50^{\circ}\text{C}$	At $t_o=5^{\circ}\text{C}$ and $t_{gc,out}=40^{\circ}\text{C}$ : 2.801	At $t_o=5^{\circ}\text{C}$ and $t_{gc,out}=40^{\circ}\text{C}$ : 16.1%
Yazawa et al. (2015) Yazawa et al. (2016)	T, O	Single-stage CO <sub>2</sub> cycle with single expansion, with thermoelectric subcooler	Single-stage CO <sub>2</sub> cycle with single expansion without IHX	$t_o=10^{\circ}\text{C}$	$t_{gc,out}=40^{\circ}\text{C}$	2.39	+22.6%
Dai et al. (2017b)	T, O	Single-stage CO <sub>2</sub> cycle with expander before receiver and thermoelectric subcooler	Single-stage CO <sub>2</sub> cycle with expander before receiver (others considered)	$t_o=-35 \text{ to } 15^{\circ}\text{C}$	$t_{gc,out}=30 \text{ to } 45^{\circ}\text{C}$	At $t_o=5^{\circ}\text{C}$ and $t_{gc,out}=35^{\circ}\text{C}$ : 3.42	At $t_o=5^{\circ}\text{C}$ and $t_{gc,out}=35^{\circ}\text{C}$ : 12.1%
Jamali et al. (2017)	T, O	Single-stage CO <sub>2</sub> cycle with two-stage thermoelectric modules in subcooler and gas-cooler	Single-stage CO <sub>2</sub> cycle with single expansion without IHX	$t_o=-10 \text{ to } 10^{\circ}\text{C}$	$t_{gc,out}=35 \text{ to } 50^{\circ}\text{C}$	At $t_o=5^{\circ}\text{C}$ and $t_{gc,out}=40^{\circ}\text{C}$ : 3.06	At $t_o=5^{\circ}\text{C}$ and $t_{gc,out}=40^{\circ}\text{C}$ : 15.9%